HAMK
Häme University
of Applied Sciences

Integrating Automation and Optimisation of Runway Components Design in Rapid Offer Creation Process of Industrial Cranes

Bachelor's thesis

Construction Engineering

Spring 2024

Piotr Rutkowski

HAMK
Häme University
of Applied Sciences

Construction Engineering Abstract
Author Piotr Rutkowski Year 2024
Subject Integrating Automation and Optimisation of Runway Components Design in Rapid Offer Creation Process of Industrial Cranes
Supervisors Ahmad Shahgordi (HAMK), Tero Aaltonen (Konecranes)

This thesis, commissioned by Konecranes, focuses on scrutinizing the equations governing the design of essential runway beam elements — clamps, support plates and end stoppers — with a particular focus on their adherence to the latest Eurocode standards. The primary objective is to ensure alignment of these equations with contemporary standards and enhance them where necessary, thereby establishing a robust foundation for integration into internal computational software dedicated to the design of said elements.

In addition, the study involves the compilation and consolidation of methods dispersed across various spreadsheets within the organization. This process entails harmonizing disparate techniques, subjecting them to a rigorous evaluation against established standards, and effecting updates where deemed necessary. Until now, the fundamental aspects of the runway design have been adequately addressed in the computational software, leaving, however, the indispensable peripheral components to be computed manually through alternative methods such as spreadsheet calculations. Consequently, the creation of manufacturing drawings necessitates a manual update with these components each time, a process that can be streamlined when automating the calculation of these elements is coupled with the parametric design capabilities inherent in Computer-Aided Design (CAD) programs.

The research methodology includes a comprehensive investigation, analysis and evaluation of existing methods and calculation tools. This scrutiny is supported by a thorough exploration of prevailing standards, with a commitment to incorporating best practices exercised by leading industry experts.

In two instances minor discrepancies were identified, having a marginal impact on final outcomes. Furthermore, one specific case prompted an extension of calculations to incorporate additional checks. The outcome of this evaluative process culminated in the creation and consolidation of analytical formulas. This development paves the way for the seamless integration of these formulas into the calculation software, significantly advancing the project.

Lastly, during this thesis considerable progress was achieved in integrating some parts of the calculations into the software, and in developing a usable (although not final) User Interface. This integration signifies a noteworthy advancement in the overall project.

Keywords Runway, steel structure, crane, support plate, clamp, end stopper
Pages 46 pages and appendices 9 pages

Contents

Table of symbols

For the purpose of this thesis, the following symbols and abbreviations apply:

Symbol	Definition
A	cross-sectional area
A_c	area of contact between support plates and lower flange
A_v	shear area
E_w	width of the cross-section of the end stopper
F_{Rd}	design weld resistance of the web weld
HEA	H-section, a typical steel profile
I	moment of inertia (second moment of area)
M_{Ed}	design value of bending moment
M_{Rd}	design value of bending moment resistance
M_{Rk}	characteristic value of bending moment resistance
SHS	square hollow section
UC	used capacity
W_{el}	elastic section modulus
W_{pl}	plastic section modulus
V_{Ed}	design value of shear force
V_{Rd}	design value of shear force resistance
V_{Rk}	characteristic value of shear force resistance
a	effective throat thickness of a weld (as in EN 1993-1-8)
b_{bar}	contact bar width
b_{cs}	width of the runway cross-section/distance between clamps
b_p	width of a support plate
b_{rail}	width of the runway's rail
f_u	ultimate strength in N/mm^2
f_y	yield strength in N/mm^2
$f_{y,red}$	reduced yield strength in N/mm^2
h	width of a profile (in inertia calculations)
h_2	height of the "hook" in a clamp
h_b	height of the buffer impact force taken from the top of the runway rail
h_k	total height of a clamp
h_p	support plate height
h_t	height from the bottom of the clamp to the top of the rail
h_w	depth of web plate
k	chamfer
l_1	width of the bottom weld in a clamp, length of a bottom weld
l_2	width of the "hook" part of the clamp, length of a top weld
l_{eff}	effective length of a weld
r	outer radius of the profile's corner
t	thickness of the profile walls

t_k	thickness of the clamp
t_w	thickness of a web plate of a profile
t_f	thickness of a flange of a profile
t_p	support plate thickness
β_w	correlation factor found in table 4.1. in EN 1993-1-8
γ_{M0}	partial factor for resistance of cross-sections
γ_{M1}	partial factor for resistance of members to instability assessed by member checks
γ_{M2}	partial factor for resistance of cross-section in tension to fracture
ε	material parameter depending on f_y
η	factor for shear area
ρ	reduction factor to determine the design value of the reduced plastic bending moment resistance making allowance for the presence of shear forces
$\sigma_\perp$	normal stress perpendicular to the weld throat
$\sigma_\parallel$	normal stress parallel to the axis of the weld
σ_{Ed}	design value of stress due to normal force
σ_{Rd}	maximum permissible stress on the material
$\tau_\perp$	shear stress in the plane of the throat perpendicular to the axis of the weld
$\tau_\parallel$	shear stress in the plane of the throat parallel to the axis of the weld

Figures

Tables

Appendices

1 Introduction

Modern engineering relies extensively on computer software and digital tools for efficient design process. There is a wide selection of general solutions readily available “off the shelf” for practically every branch of engineering (such as simulation engines, CAD software, BIM systems) which over the years became indispensable for most companies. However, occasionally companies decide to develop their own tools “in house” when e.g. the needs are very industry-specific, relate to proprietary technology, rely on internal know-how or on own products. A major advantage of this approach is maintaining full control over the development of the software, its features and prioritisation.

In Konecranes, the company commissioning this thesis, both approaches are present. The company uses e.g. general-purpose CAD and simulation programs, but also maintains a large ecosystem of internal, highly specialised calculation and configuration tools. The need to expand capabilities of one of such tools – KC Runway – resulted in commisioning and development of this thesis.

1.1 Konecranes

Konecranes is a globally recognized name in the industrial sector. It holds a prominent position in the market for its expertise in lifting equipment and associated services.

Established over a century ago as Kone (“machine” or “engine” in Finnish), in 1994 it was split into two independent entities: Kone, focusing on elevator equipment and services, and Konecranes, specializing in the design, manufacturing, and maintenance of cranes, hoists, and related equipment and services (Konecranes, 2024)

Konecranes provides a large variety of comprehensive lifting solutions for a number of diverse industries. Typically, each solution involves a crane that can be classified as one of the following:

- Overhead Cranes:
  The supporting structure of the crane (runway) is fixed in place, for example by being attached to walls or columns. The crane itself runs on top of (or hangs from) the runway beam. Cranes with a single overhead girder are suitable for light to medium duty lifting applications, whereas for heavy-duty lifting tasks typically a double girder crane is required (Figure 1).

- Gantry Cranes:
  Rubber Tired Gantry (RTG) and Rail Mounted Gantry (RMG) Cranes are mobile cranes running on a supporting structure with wheels, typically used in port solutions and outdoor environments for intermodal container handling.

- Jib Cranes:
  These are smaller, stand-alone cranes fixed in place with an arm that can rotate, used in specific areas, for instance at a workstation in a factory. This type of a crane can be free standing or wall-mounted.

- Container Handling Equipment, further divided into:
  Ship-to-Shore (STS) Cranes: large cranes used for loading and unloading containers from ships in port terminals;
  Straddle Carriers: designed for the transportation and stacking of containers in port and terminal environments.

- Special Cranes:
  These cranes are designed per very specific requirements, for instance to operate in an unusually harsh environment (steel plant, nuclear power plant) or to handle exceptionally heavy loads.

In addition, there are two main approaches in the industry, which influence how each crane is designed, customised and manufactured:

- Engineered to Order (ETO):
  In this approach, each product is uniquely designed to meet individual needs and specifications of a customer. The special requirements can, for instance, relate to lifting capacity, special operating condition, integration with existing structures, extended wear and tear or additional custom features. This approach allows for highly customised solutions while sacrificing the design duration and costs.

- Configured to Order (CTO):
  As the name suggests, the crane is configured and assembled from pre-defined modules, components and parts to create a product that fulfils the customer’s requirements. These solutions are more standardized and cover a variety of most usual scenarios with typical features and options. Some level of customisation is still possible

but usually from predetermined options. The rapid design process often results in a more economical solution overall.

It must be noted that these two classification types are fundamentally independent of each other, meaning that theoretically any type of crane can be designed using either ETO or CTO approach. However, in practice it is more typical that only the most common, more standard crane types are designed as CTO, such as overhead cranes and gantry cranes. (Konecranes, internal documentation, n.d.)

When designing cranes and their supporting structures, it is important to adhere to the correct standards. Since a typical overhead crane assembly contains both mobile elements (e.g. trolley) and fixed elements (e.g. runway, columns) it is crucial to distinguish which parts are considered machinery and which are construction products. These matters are regulated in the following documents:

- The EU Machinery Directive 2006/42/EC (Directive on machinery 42/EC/2006, 2006): all mobile parts of the crane.

- Construction Product Regulations 305/2011 (Regulation (EU) No 305/2011 of the European Parliament and of the Council of 9 March 2011 laying down harmonised conditions for the marketing of construction products, 2011): typical runways fixed in place to building's structural elements, with exception of light crane systems (free-standing or not), which are regulated under a separate standard (EN 16851:2017 + A1:2020:en, 2020).

Figure 1. Top running, double girder overhead crane (Konecranes, 2016).

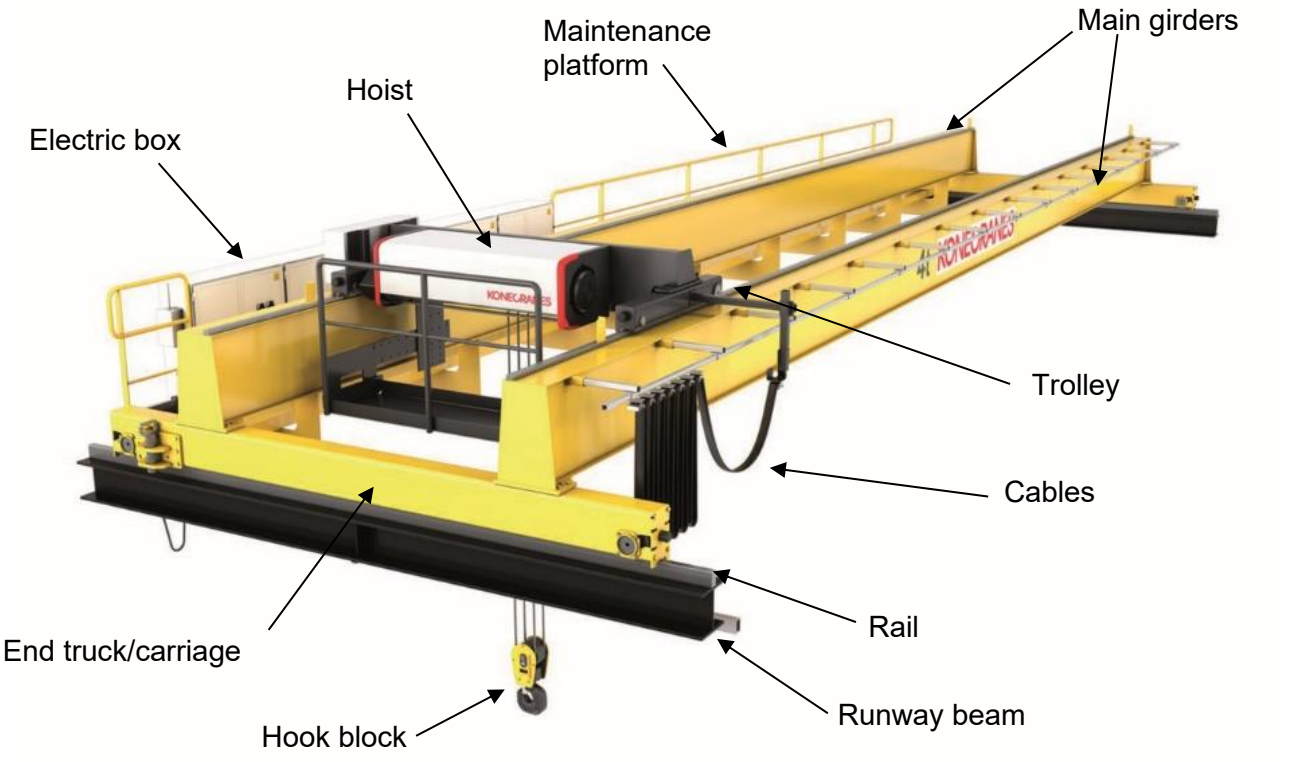

One of Konecranes' distinguishing features lies in its emphasis on technological innovation. The company has continuously invested in research and development to introduce advanced automation, digitalization, and predictive maintenance solutions to its portfolio. Such initiatives not only underscore Konecranes' commitment to safety and sustainability in material handling processes but also enhance operational efficiency.

Development of internal software calculation tools is a direct consequence of the company's strategy to invest in technological innovation as a way to achieve that efficiency and stay ahead of the competitors.

1.2 KC Runway and Calculation Tools

KC Runway calculation software is a part of the Calculation Tools ecosystem managed and developed internally by Konecranes. Other tools include, for instance, KC Girder, KC Rope, KC Gantry etc., each developed to target a specific engineering task. These tasks might be related to the crane load bearing structure, but also machinery selection, rope reeving, electrical systems, and others. Where applicable, the results from one application might be fed as an input to another one. (Konecranes, internal documentation, n.d.)

Primarily, these tools are used by the engineers and sales representatives to rapidly and efficiently provide offers of new cranes to the potential customers in a streamlined sales process, including a realistic price estimation and eventually manufacturing drawings. However, they can also be used individually and independently as stand-alone applications, for instance in cases such as repairs, upgrades, or modernisations of existing cranes to examine stability and safety of components in question. (Konecranes, internal documentation, n.d.)

As such, KC Runway is a vital part of the whole process and should be automated and streamlined as much as possible, while still leaving the user a level of control detailed enough to cover existing structures when needed. Konecranes sells several hundreds of runways per year in Europe alone and the intention is to increase the sales there further, as well as in other markets.

Currently, it is possible to calculate several parameters related to the runway's main beams, such as the beams' profiles in each span, their deflections, used capacities and support reactions at each joint. However, various elements vital for the final design and delivery are missing from the calculations, meaning that they need to be calculated manually for each order and added to the final design and drawings. That, of course, adds costs, extends the design time and makes cost estimation in the sales phase inaccurate. Those elements include:

- buffer end stoppers
- support plates at the joints
- clamps at the consoles

Extending the capabilities of KC Runway by adding the abovementioned features and automated calculations would noticeably speed up the design process of runways.

2 Scope of this thesis

Proposing a solution that will allow adding the runway structural elements to KC Runway and thus streamlining the offer creation process is the main focus of this thesis. That includes analysing these elements in detail for different use case scenarios, analysing existing designs and choosing most suitable ones, providing the necessary mathematical calculations in accordance with the relevant standards to ensure safety, creating optimisation algorithms where it is reasonable, and implementing those calculations in KC Runway to some degree.

From the user experience perspective, a final, fully functional solution is not expected at this stage, as this thesis is only a part of a larger project to expand the capabilities of KC Runway. The user interface and final architecture of the software will be done in a separate study.

The scope of the thesis includes:

- most common types of CTO cranes for European market
- European standards (see References)
- top running cranes (as opposed to underhung)
- console supported (as opposed to columns)
- most common designs with certain assumptions (SHS or RHS sections used as the end stoppers, clamps mounted in line with the support plates)

The overall goal of the thesis is to streamline and automate the design process, to design, improve, standardize and automate calculations, and to implement the best practices and experience accumulated over the years within Konecranes directly into the application.

3 Methodology

The research methodology includes a comprehensive investigation, analysis and evaluation of existing methods used internally in the organization, available calculation tools and consultations with company subject matter experts. It is anchored in the European standards, internal documentation, previous designs, company know-how and accumulated experience within Konecranes.

As the first step, designs currently used within Konecranes were gathered and analysed. They varied across different countries or regions, sometimes to a great degree, so for the implementation it was important to select the designs that are generic enough to support most cases. Next, calculation methods, procedures or technical manuals existing within Konecranes for the selected designs were analysed, focusing especially on their base assumptions and compliance with the latest standards. Where discrepancies or shortcomings were found, they were updated and/or extended. It must be noted that the resulting findings do not necessarily mean that previously used methods were false, incorrect or otherwise unsound – rather that e.g. the standards they were based on were updated or that the calculations could be extended thanks to the possibilities of KC Runway and custom programming. Naturally, each design and related calculation procedures were consulted with the company senior designers and the thesis supervisors, and eventually approved by Konecranes chief designer, Kari Siitari.

In parallel to this process, a prove of concept of the application was systematically being developed. It was necessary because translating the calculation methods into a working software presents unique challenges that were not obvious at the beginning of the project.

4 The runway details

In all the calculation examples in this chapter, default values of loadings from KC Runway were used, unless specified otherwise. The numerical results are not as relevant as the equations themselves, and theories and codes they are based on.

4.1 End stoppers

4.1.1 General info and purpose

End stoppers are structures typically installed at the very ends of the runway to limit the maximum travel of the end carriages in an emergency situation (Figure 2). It is vital to note that they are not to be relied on during a normal use of the crane, as there are other systems in place to slow down and stop the crane before it reaches the end of the runway. However, if any of those systems were to fail, the end stoppers are meant to receive the impact from the traveling crane (specifically from the end buffers of the end carriage) and prevent its derailing and falling off the runway.

They can have many forms but among the most typical and cost-efficient solutions is welding vertically a hollow section profile to the runway's top flange. In Finland, the most common choice is Square Hollow Section (SHS).

A 3D model of an end stopper made from an SHS profile installed on HEA profile runway beam is visible in Figure 3.

This type of the end stopper typically has two inclined cuts (visible in the 3D model and in Figure 4 between the flange and the rail) made to accommodate the rail going through it. This is not strictly necessary because it would be possible to shorten the rail and weld the end stopper directly to the flange around the whole cross section. However, during the life span of the crane it is sometimes required to reposition the end stopper (for example in case of layout changes on the factory floor) which this design allows easily. Moreover, it represents the "worst case scenario" with the minimal area available for welding thus making it more conservative.

Figure 2. A cross-section of a runway with an end stopper visible and an end buffer on an end carriage.

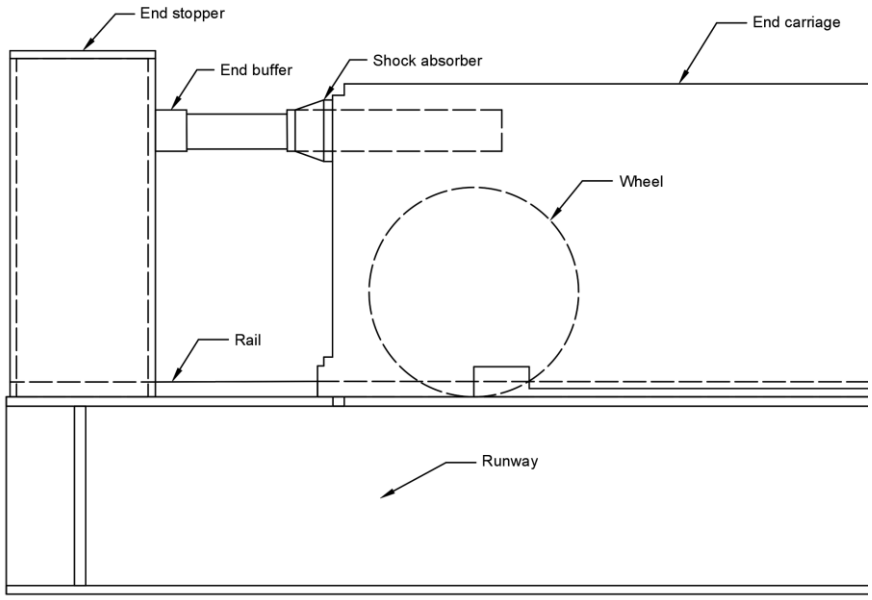

Figure 3. A 3D model of a runway beam with an end stopper, rail, support plate and clamps visible.

4.1.2 Loadings involved

The dimensioning force in case of the end stoppers is the buffer collision force, which mainly depends on the crane's own dead weight and the dead weight of the hoist. The maximum collision force is calculated by KC Girder and is then imported into KC Runway, or it can be manually defined by the user.

Geometry check

In order to achieve full automation, some profiles have to be rejected already based on a simple geometry check. Namely, it is possible that some profiles are either too wide for the runway's flange, or too narrow for the rail. In such a case, all other calculations are skipped, and the profile is marked as unsuitable.

Buckling check

According to the relevant standard (EN 1993-1-1:2022en, 2022, p. 66), the shear buckling resistance of the webs needs to be checked according to standard 1993-1-5 if the following condition applies:

$$\frac{h_w}{t_w} > 72 * \frac{\varepsilon}{\eta} \quad (1)$$

Consequently, if the above condition does not apply, it is assumed that the shear buckling is not the limiting factor, so for simplicity the application should only allow the profiles not passing this condition. ε is defined as a square root of 235 divided by the yield strength in MPa, whereas factor η can be assumed as 1.2 for steel grades up to and including S460, for higher strengths η should be taken as 1.0 (EN 1993-1-1:2022en, 2022, p. 66).

Bending resistance

The requirements for the bending resistance are given in the Eurocode 1993-1-1 (EN 1993-1-1:2022en, 2022, p. 63). It specifies that the ratio of the design bending moment M_{Ed} to the design resistance M_{Rd} at each cross-section shall be smaller than or equal to 1:

$$\frac{M_{Ed}}{M_{Rd}} \leq 1 \qquad (2)$$

M_{Rd} is obtained from the characteristic value of the bending moment resistance M_{Rk} after reducing it by the factor γ_{M0}. In accordance with the table found in chapter 8.2.2.6 of the standard (EN 1993-1-1:2022en, 2022, p. 61), M_{Rk} depends on the cross section's section modulus W for each axis, which in turn depends on the class of the cross section. For the end stoppers, the exact class is not calculated, but it is checked indirectly that the cross section is at least class 3. Therefore elastic section modulus W_{el} is used (Table 1).

Table 1. Section areas and section moduli for all cross-section classes.

Class	1	2	3	4
Section area A_i	A	A	A	A_{eff}
Section modulus W_y	$W_{pl,y}$	$W_{pl,y}$	$W_{el,y}$[a, b]	$W_{eff,y}$[b]
Section modulus W_z	$W_{pl,z}$	$W_{pl,z}$	$W_{el,z}$[a, b]	$W_{eff,z}$[b]

Consequently, the characteristic bending moment resistance, M_{Rk}, is calculated according to:

$$M_{y,Rk} = W_{el} * f_y \qquad (3)$$

where f_y is the yield strength of the material and $W_{el,y}$ is the elastic section modulus.

Figure 4. The buffer end stopper at the end of a runway with visible welds locations (in red) and acting forces and reactions (arrows).

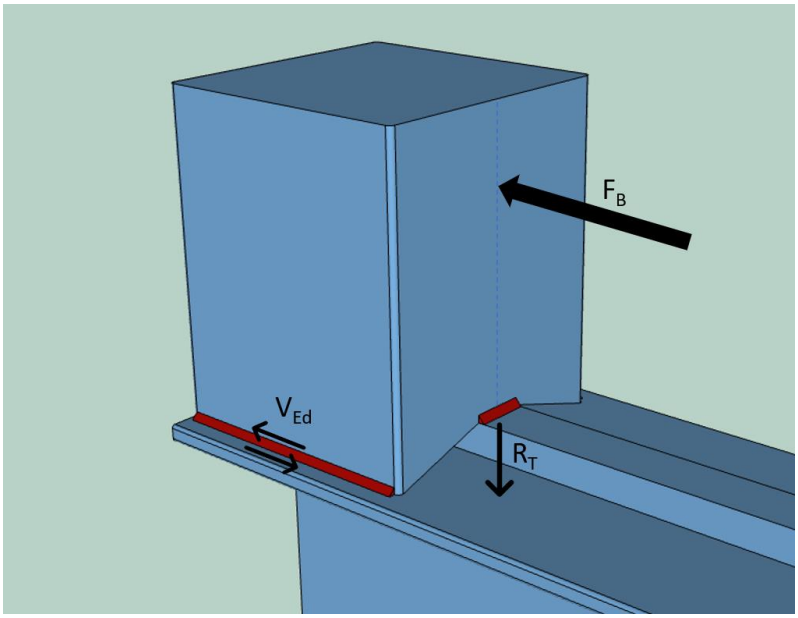

Figure 5. A section of an end stopper with symbolical dimensions and forces.

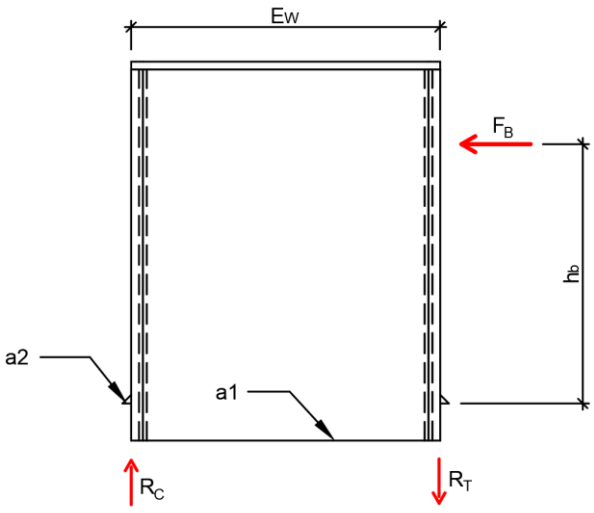

The section modulus, W, and the moment of inertia, I, are usually given in the geometrical properties of the standard cross sections, but in the case of the SHS end stoppers, they need to be calculated. The reason is that the SHS profile is not welded at its whole perimeter. Instead, the webs are welded to the runway beam's top flange, and parts of the end stopper flanges are welded to the rail (marked in red in Figure 4). In addition, the buffer end stopper under the buffer force acts as a cantilever, meaning that the maximum bending moment will

be at its base and therefore only the effective (“active”) part of the cross section should be considered. The equation to conservatively calculate the moment of inertia:

$$I = 2 * \frac{t * (h - 2 * r)^3}{12} + 2 * \left(\frac{b_{rail} * t^3}{12} + t * b_{rail} * \left(\frac{h - t}{2} \right)^2 \right) \quad (4)$$

Where:

t is the thickness of the profile walls

h is the width of the profile

b_{rail} is the width of the runway’s rail

r is the outer radius of the profile’s corner

However, in cases where smaller beams are used for the runway, it could be argued that the thinner flanges do not provide enough stiffness for the end stopper flanges to be effective, further reducing the active area. Appendix 1 shows an additional check that can be preformed in such cases.

Next, the section modulus can be calculated:

$$W_{el} = \frac{I}{d} \quad (5)$$

The characteristic bending moment resistance, M_{Rk}, can be calculated according to eq. (3), and the design bending moment resistance, M_{Rd}, is obtained with γ_{M0}: (specific values and explanations of factors γ can be found in the Appendix 1):

$$M_{Rd} = \frac{M_{Rk}}{\gamma_{M0}} \quad (6)$$

Finally, the used capacity can be calculated:

$$UC = \frac{M_{Ed}}{M_{Rd}} \tag{7}$$

Shear resistance

The requirements for the shear resistance are given in chapter 8.2.6 of the same standard (EN 1993-1-1:2022en, 2022, p. 64). It is given that the design value of the shear force V_{Ed} shall be equal or smaller than the design shear resistance V_{cRd} :

$$\frac{V_{Ed}}{V_{cRd}} \leq 1 \tag{8}$$

Where V_{Ed} is the dimensioning shear force dependent on the buffer impact force.

Since torsion is not present, the design plastic shear resistance $V_{pl,Rd}$ can be used and is calculated according to:

$$V_{pl,Rd} = \frac{A_v(f_y/\sqrt{3})}{\gamma_{M0}} \tag{9}$$

Where A_v is the shear area. In case of square hollow sections (SHS) the shear area is defined as:

$$A_v = A * h/(b + h) \tag{10}$$

Where A is the cross-sectional area and $b{=}h$ is its height and depth.

Lastly, the used capacity can be calculated:

$$UC = \frac{V_{Ed}}{V_{plRd}} \tag{11}$$

Combined bending and shear

Because the bending moment and the shear force coincide at the same cross section, their combined effects need to be checked as well. Specifically, the reduction of the bending moment resistance due to the shear force:

$$\frac{M_{Ed}}{M_{V,Rd}} \leq 1 \tag{12}$$

Where $M_{V,Rd}$ is the design plastic bending moment resistance reduced due to the shear force V_{Ed}. This effect can be neglected if the design shear force V_{Ed} is at most half of the plastic shear force resistance of the cross section. Otherwise, equation (12) must be proven using reduced yield strength of the material so that:

$$f_{y,red} = (1 - \rho) * f_y \tag{13}$$

where

$$\rho = \left(\frac{2 * V_{Ed}}{V_{c,Rd}} - 1\right)^2 \tag{14}$$

while $V_{c,Rd}$ is taken as the plastic shear resistance, eq. (9) (EN 1993-1-1:2022en, 2022, pp. 68, 69).

Welds resistance

As shown in Figure 4, the end stopper is welded along the whole length of its webs to the runway (further called the web weld), and partially to the rail (further called the flange weld). It is assumed that the former weld takes only the shear force, and the latter weld takes only the vertical forces (i.e. tension/compression pair) resulting from the buffer collision. It is also assumed that the runway's top flange is stiff enough to take all the tension and compression because of the presence of the rail, which is much stiffer than the flange alone. However, in more extreme cases (e.g. buffer collision forces > 50kN) additional stiffeners are needed under the end stopper.

According to the standard, it must be checked that the effective length l_{eff} of the weld is sufficient, especially in case of the end stopper-to-rail weld since it might be very short. The effective length can be taken as the overall weld length l reduced by twice the throat thickness a. The code also specifies that the minimum effective length must be 30mm or 6 times the throat thickness. Thus, the minimum *effective* length of a weld is 30mm, whereas the absolute minimum *total* length (i.e. the minimum length of the part welded) is 36mm (EN 1993-1-8:2005, 2005, p. 42):

$$l_{min} = \min(30mm, 6 * a) \tag{15}$$

$$l_{eff} = l - 2 * a \tag{16}$$

The rails offered by Konecranes in the standard solutions are at least 50mm so this requirement will be typically fulfilled. However, it is theoretically possible that the weld is too short, for example when using the tool in renovation projects to calculate capacities of an existing, old runway. In such cases, relevant information should be presented to the user and the decision left to the engineer in charge of the design.

The Eurocode permits two methods for calculating the welds: directional and simplified (EN 1993-1-8:2005, 2005, pp. 43, 44). The directional method is chosen for this part of the project because it tends to give more accurate results (Kubicki, 2021).

In this method, the stresses acting on the weld are split into components parallel and perpendicular to the throat plane and then combined so that:

$$\sqrt{\sigma_{\perp}{}^2 + 3 * (\tau_{\perp}{}^2 + \tau_{\parallel}{}^2)} \leq \frac{f_u}{\beta_w \gamma_{M2}} \qquad \text{and} \qquad \sigma_{\perp} \leq 0.9 * \frac{f_u}{\gamma_{M2}} \qquad (17)$$

where f_u is the ultimate tensile strength of the weaker part and β_w is the correlation factor from Table 2.

Table 2. Correlation factor for fillet welds

Standard and steel grade			Correlation factor β_w
EN 10025	**EN 10210**	**EN 10219**	
S 235 S 235 W	S 235 H	S 235 H	0,8
S 275 S 275 N/NL S 275 M/ML	S 275 H S 275 NH/NLH	S 275 H S 275 NH/NLH S 275 MH/MLH	0,85
S 355 S 355 N/NL S 355 M/ML S 355 W	S 355 H S 355 NH/NLH	S 355 H S 355 NH/NLH S 355 MH/MLH	0,9
S 420 N/NL S 420 M/ML		S 420 MH/MLH	1,0
S 460 N/NL S 460 M/ML S 460 Q/QL/QL1	S 460 NH/NLH	S 460 NH/NLH S 460 MH/MLH	1,0

Conservatively, it can be assumed to be 1.

In line with the initial assumptions, the flange weld of the end stopper takes the whole resulting tension. An outline of that weld with the stresses split into components is presented in Figure 6.

Figure 6. A model of the flange weld with component stresses.

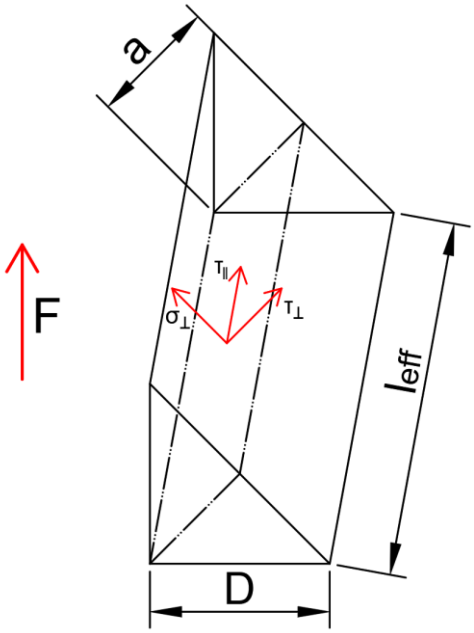

It can be assumed that the stresses $\sigma_\perp$ and $\tau_\perp$ are at 45-degree angle α in relation to F and therefore:

$$\sigma_\perp = \tau_\perp = \frac{F * sin\alpha}{a * l_{eff}} = \frac{F}{\sqrt{2} * a * l_{eff}} \tag{18}$$

Shear stress parallel to the throat axis $\tau_\parallel$ is zero. From simple static analysis it is known that:

$$F = \frac{F_B * h_b}{E_W} \tag{19}$$

The eq. (17) in case of the flange weld simplifies to:

$$\frac{2F_B * h_b}{a * l_{eff} * E_w * \sqrt{2}} \leq \frac{f_u}{\beta_w \gamma_{M2}} \tag{20}$$

It is also possible to calculate the utilisation ratio of a default weld thickness as well as the minimal weld needed a_{min}

$$UR = \frac{2F_B * h_b * \beta_w \gamma_{M2}}{a * l_{eff} * E_w * \sqrt{2} * f_u} \tag{21}$$

$$a_{min} = \frac{2F_B * h_b * \beta_w \gamma_{M2}}{l_{eff} * E_w * \sqrt{2} * f_u} \tag{22}$$

Analogously, it is assumed that the web weld takes the whole shear force and no perpendicular stresses are present. This situation is depicted symbolically in Figure 7. Consequently, the equation (17) for the web weld simplifies to:

$$\frac{F_B * \sqrt{3}}{a * 2 * l_{eff}} \leq \frac{f_u}{\beta_w \gamma_{M2}} \tag{23}$$

Finally, the utilisation ratio and the minimum weld size are obtained as follows:

$$UR = \frac{F_B * \sqrt{3} * \beta_w \gamma_{M2}}{a * 2 * l_{eff} * f_u} \tag{24}$$

$$a_{min} = \frac{F_B * \sqrt{3} * \beta_w \gamma_{M2}}{2 * l_{eff} * f_u} \tag{25}$$

Figure 7. A model of the web weld with component stresses.

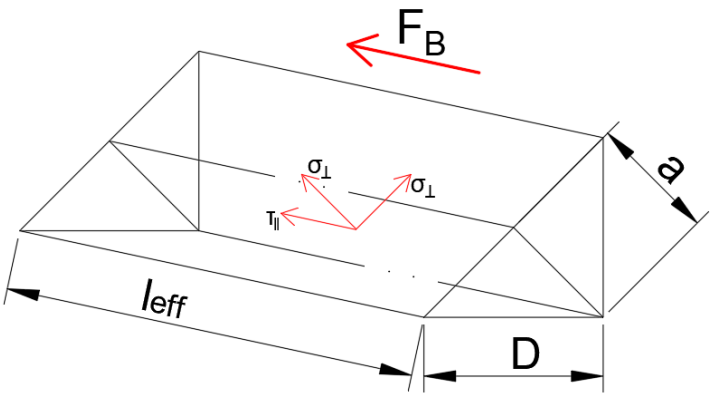

4.1.3 Optimisation and automation

The application allows to define an end stopper on either end of the runway independently. The reason is that sometimes it is useful to calculate just part of the runway, in which case the end carriage needs to be able to travel beyond the end of the defined runway beam.

The application can automatically select the smallest runway profile fulfilling the projects parameters. It is done so that during loading of the available profiles from the database, they are sorted by the profiles' mass, from the lightest to the heaviest. Then, the algorithm runs all the calculations for each profile starting from the smallest and selects the first profile for which all checks are passed.

In addition, there is an option to manually choose a profile to be checked against all the calculations.

4.1.4 Results

The implemented calculations and the UI for selecting the end stoppers in KC Runway is shown in case of successful automatic optimisation in Figure 8, and failed manual check in Figure 9. It must be noted that the UI is not final and serves only as a proof of concept for the calculations and optimisation.

Figure 8. Automatic selection of the smallest suitable profile from all available in the database.

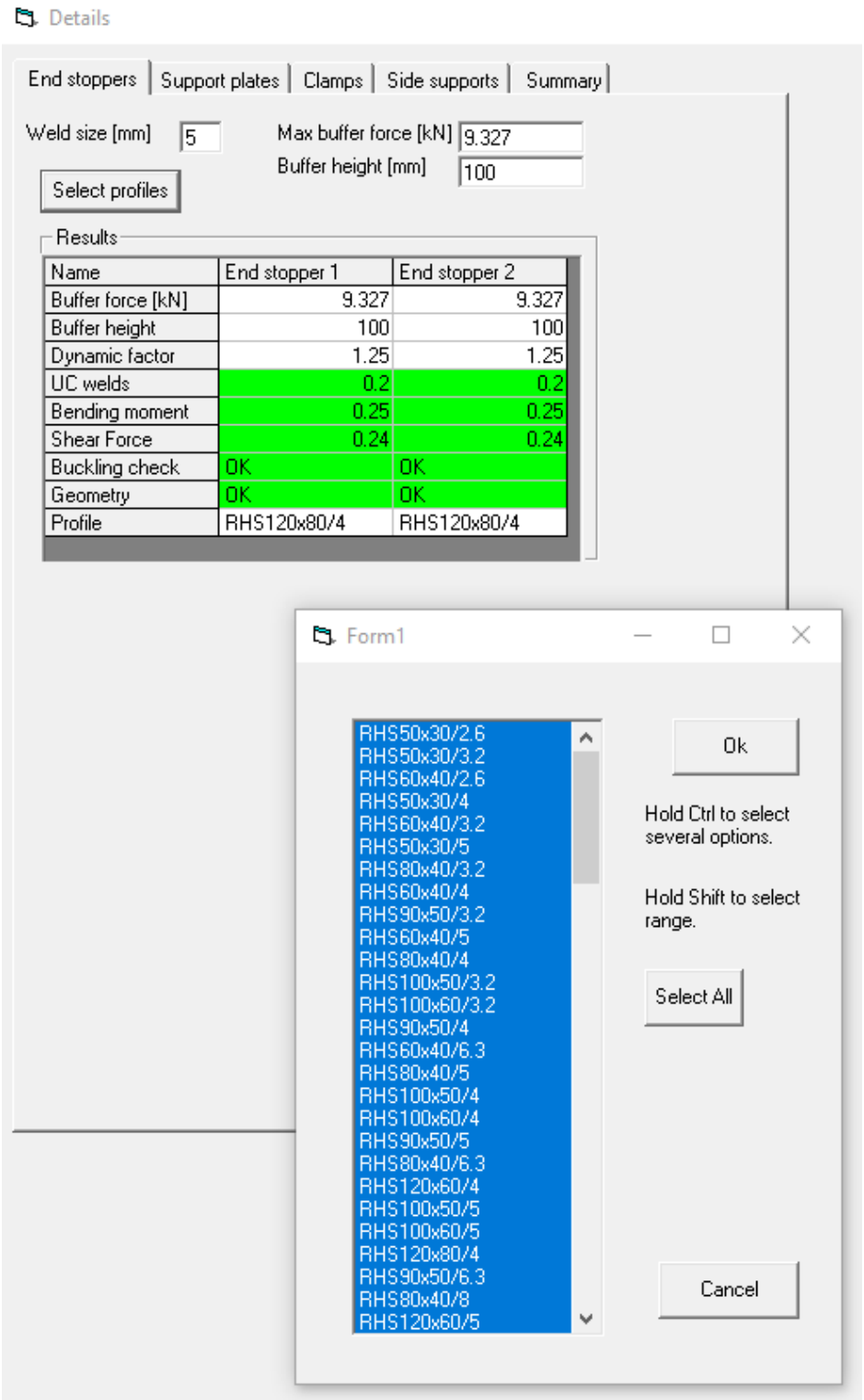

Figure 9. Failed check after selecting a specific profile manually.

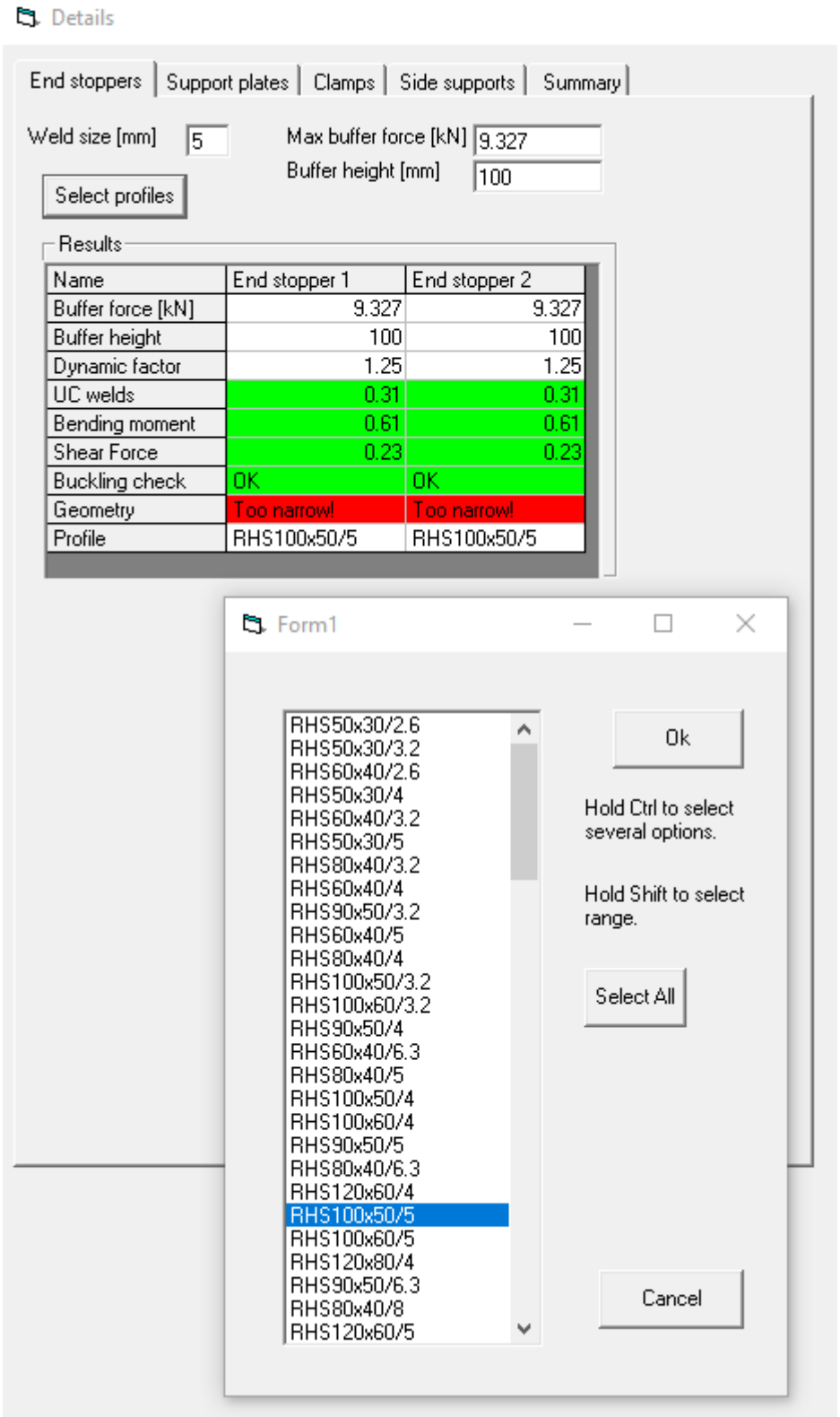

4.2 Support plates

4.2.1 General info and purpose

A cross-section of a runway beam with the support plates and other elements is presented in Figure 10. Support plates are installed at the runway's support locations (consoles or columns) for several reasons, depending on specific design requirements, but among typical reasons are:

- to transfer the horizontal forces to the clamps; otherwise, the entire bending moment from the horizontal force would be taken only by the web, which could fail due to small inertia in *z* direction

- to prevent the web from buckling under heavy vertical load

- to spread the vertical load onto a bigger area and effectively transfer it to the contact bar under the runway

- to prevent shear buckling at the supports (EN 1993-1-1:2022en, 2022, p. 66), (EN 1993-1-5, 2006, p. 21)

Figure 10. Runway cross section with rail, support plate and clamps visible.

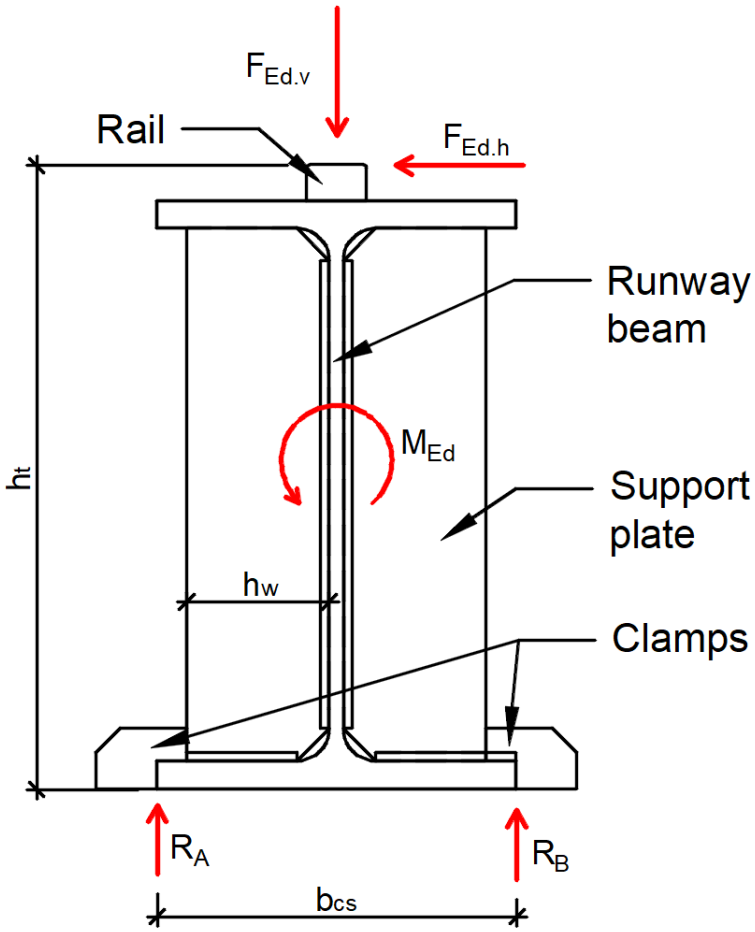

4.2.2 Design types

In case of a welded runway, where the beams connections at the supports are capable of transferring moments, one pair of support plates is sufficient (one plate on each side of the runway web). In case of a hinged connection, a set of two is required, one pair per beam, i.e. on each side of the joint. In addition, currently in KC Runway it is possible to define two beams of different sizes connected at a joint (Figure 11). For this reason, even in case of a fixed connection, it is important to calculate the plates twice per every joint – for each beam separately - because the dimensions of the beam dictate the maximum dimensions of the plate.

Figure 11. Two beams with different sizes defined in KC Runway.

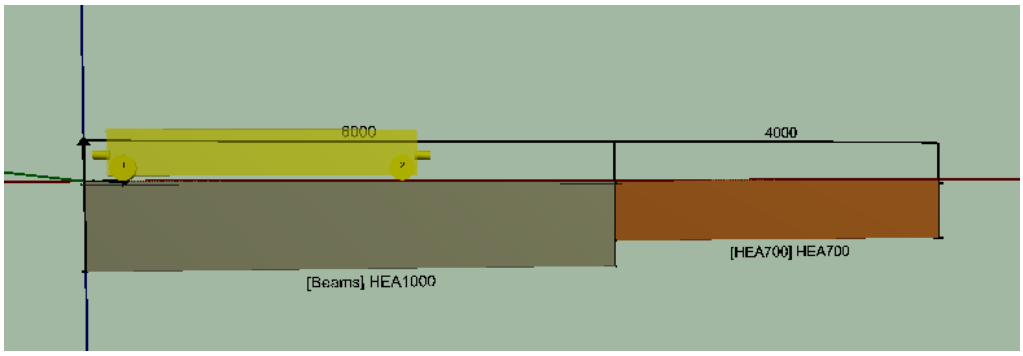

In such a case, it is up to the designer to decide if the support should be located under the bigger beam, or under the smaller one. It must be noted that even though such a geometry is technically possible in the software, in practice there would be an inclined transition section between the two beams.

4.2.3 Calculations

Surface pressure between the contact bar and the runway profile

The surface pressure/bearing capacity is calculated at the bottom of the support plates in accordance with the effective length for the resistance to transverse forces as stated in chapter 8.2.11 of the Eurocode 1993-1-1 (EN 1993-1-1:2022en, 2022, p. 75). Conservatively, the area under the plate directly in contact with the bottom flange is considered, as well as the assumed area of force transfer between the flange and the bottom contact bar, spread through the flange thickness at approximately 45 degree angle (Figure 12).

Figure 12. Schematic distribution of vertical force under the runway web and through the flange, a cross section through the runway.

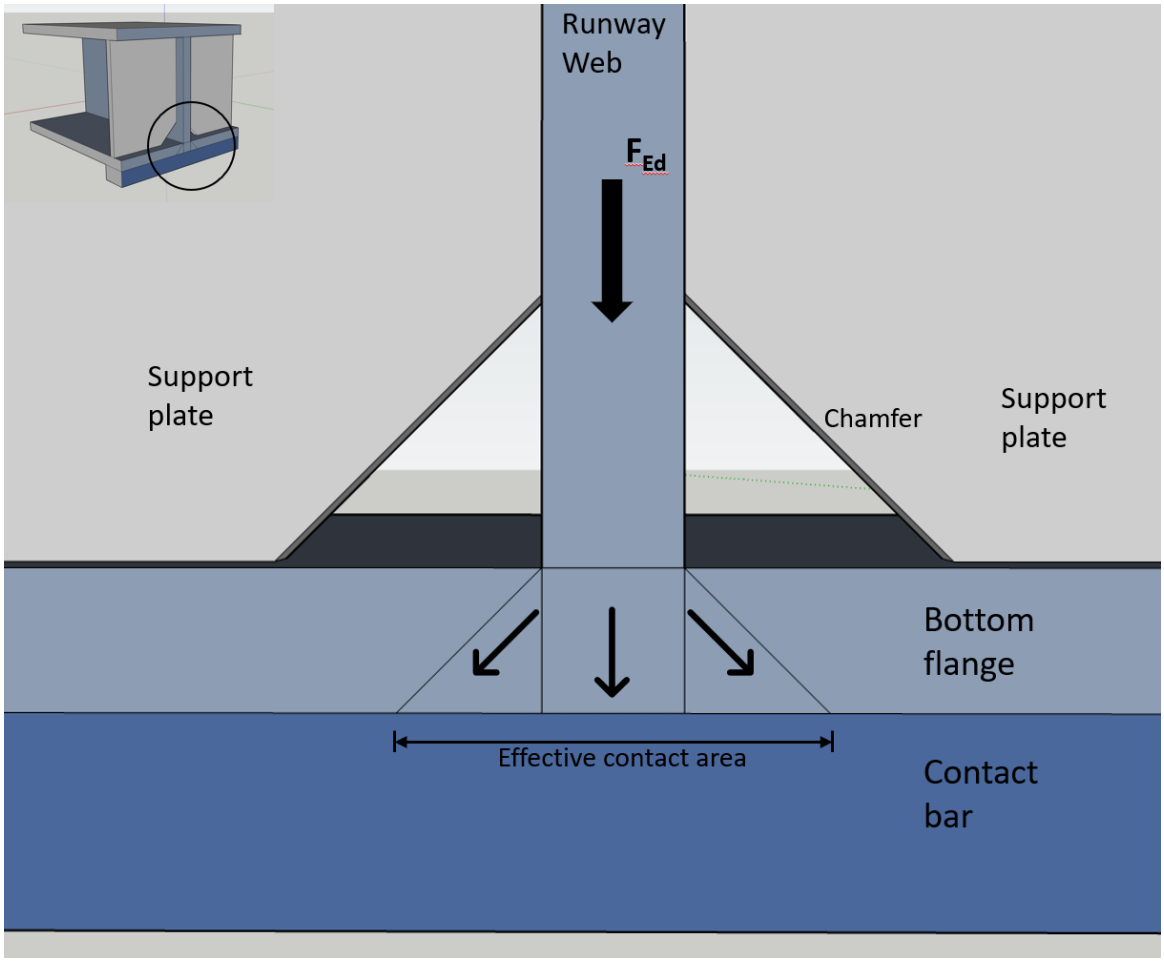

First, the maximum permissible surface pressure is calculated from the material's properties including appropriate partial factor:

$$\sigma_{Rd} = \frac{f_y}{\gamma_{M0}} \tag{26}$$

Following, the area of the contact is calculated, as explained earlier:

$$A_c = b_{bar} * \left(t_w + 2 * t_f\right) + \left(b_p - k\right) * t_p * 2 \tag{27}$$

Finally, the design stress and the used capacity are calculated:

$$\sigma_{Ed} = \frac{F_{Ed}}{A_c} \tag{28}$$

$$UC = \frac{\sigma_{Ed}}{\sigma_{Rd}} \tag{29}$$

Capacity of the web weld and the bottom weld

The welds are calculated in accordance with the simplified method given in Eurocode 3 (EN 1993-1-8:2005, 2005, p. 45). Even though in reality the stress distribution along the length of the weld is most likely not exactly uniform, the standard EN 13001-3-1 allows to consider it as uniform (EN 13001-3-1:2012 + A2:2018, 2012, p. 20).

The design weld resistance of the web weld, F_{Rd}, is calculated with the weld area (thickness a_1 times the length of the weld which is the web height reduced by the chamfers) and reduced ultimate strength of the weld material. In the used capacity, the vertical force is divided by double weld resistance F_{Rd} because there are two plates – one on each side of the web.

$$A_{weld} = 2 * a_1 * \left(h_p - 2 * k\right) \tag{30}$$

$$F_{w.Rd} = A_{weld} * \frac{\left(\frac{f_u}{\sqrt{3}}\right)}{\beta_w * \gamma_{M2}} \tag{31}$$

$$UC = \frac{F_{Ed.v}}{2 * F_{w.Rd}} \tag{32}$$

Similarly, the capacity of the bottom weld is calculated as follows, where the length of the weld is taken as the web's width reduced by the chamfers:

$$A_{weld} = 2 * a_2 * (b_p - k) \tag{33}$$

$$A_{web} = t_w * b_{bar} * 2 \tag{34}$$

$$F_{w.Rd} = 2 * A_{weld} * \frac{\left(\frac{f_u}{\sqrt{3}}\right)}{\beta_w * \gamma_{M2}} + A_{web} * \frac{f_y}{\gamma_{M2}} \tag{35}$$

$$UC = \frac{F_{Ed.v}}{F_{w.Rd}} \tag{36}$$

It must be noted that when calculating the ability of the weld to transfer the forces, the ultimate strength of the material is used for the welds and yield strength for the runway beam web.

It is worth mentioning that in the equations currently used at Konecranes, the result is even more conservative because it also includes γ_{M0} instead of β_w, which the code does not. As a result, the calculated capacity of the weld is a bit lower (i.e. the used capacity is 12% higher), leading to a more conservative design.

It is important to ensure the quality of the welds, especially when thicker plates are used. According to the industry recommendations (SSAB, 2019), preheating might be required to prevent cracks. The need of preheating mainly depends on the thickness of the welded plates because the more material is present the higher the heat capacity which impacts the cooling temperature of the weld in a major way. If the weld is cooled too quickly, it might not achieve the required strength by becoming too brittle and/or cracking. The detailed recommendations are given in the European welding standard. (EN 1011-2, 2001)

Bending stress of the support plates

Bending stress comes from the horizontal force applied to the rail, on the top of the beam's cross section. It is due to acceleration and deacceleration of the crane in transverse and longitudinal directions, and skewing forces.

First, elastic section modulus W_{el} of the cross-section responsible for resisting the bending moment is calculated:

$$W_{el} = \frac{t_p}{6} * \left(t_w + 2 * b_p\right)^2 \tag{37}$$

Following with the design stress and allowable stress calculations:

$$\sigma_{td} = \frac{F_{Ed.h} * h_t + M_{Ed}}{W_{el}} \tag{38}$$

$$\sigma_{all} = \frac{f_y}{\gamma_{M0} * \gamma_{M2}} \tag{39}$$

Lastly, the utilisation ratio can be calculated:

$$UR = \frac{\sigma_{td}}{\sigma_{all}} \tag{40}$$

Lateral buckling check of the support plates

The buckling check is based on the profile classification and is meant to provide a simple way to ensure buckling prevention. Namely, as stated in Eurocode 1993-1-1 chapter 7.5.2.: "class 3 cross-sections are those in which the stress in the extreme compression fibre of the steel member assuming an elastic distribution of stresses can reach the yield strength, but local buckling is liable to prevent development of the plastic bending moment resistance" (EN 1993-1-1:2022en, 2022, p. 51). In plain English it means that the class 3 cross section can reach its

elastic limit, but local buckling will prevent it from reaching its plastic limit (i.e. local buckling of the plate will occur before its plastic limit is reached).

The plate is considered a “free end” in pure compression and so the column 2 from Table 3 can be applied and the following relationship checked:

$$\frac{b_p}{t_p} < 14 * \sqrt{\frac{235\ [MPa]}{f_y}} \tag{41}$$

Table 3. Maximum width-to-thickness ratios for compression parts of outstanding flanges (EN 1993-1-8:2005, 2005, p. 53).

Outstand flanges			
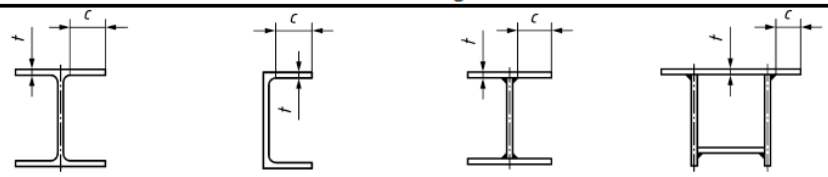 Rolled sections		Welded sections	
	Part in pure compression	Part subject to bending and axial force	
Stress distribution in parts (compression positive)		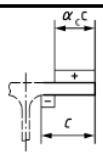	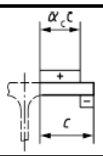
Class 1	$c/t \le 9\,\varepsilon$	$c/t \le \frac{9\varepsilon}{\alpha_c}$	$c/t \le \frac{9\varepsilon}{\alpha_c\sqrt{\alpha_c}}$
Class 2	$c/t \le 10\,\varepsilon$	$c/t \le \frac{10\varepsilon}{\alpha_c}$	$c/t \le \frac{10\varepsilon}{\alpha_c\sqrt{\alpha_c}}$
Stress distribution in parts (compression positive)	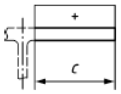	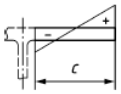	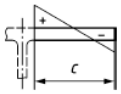
Class 3	$c/t \le 14\,\varepsilon$	$c/t \le 21\,\varepsilon\sqrt{k_\sigma}$ For k_σ see EN 1993-1-5	

4.2.5 Results

Figure 13 shows the support plates calculations implemented into KC Runway. The basic input data are the same for all the plates. The software checks the plate's dimensions against every joint and increases the plates thickness if necessary (from those defined and available in the database). The used capacities vary because the loads might differ between the joints. In the case presented in the figure, the smallest thickness available was sufficient. In addition, the position of each plate pair is indicated (joint, member and cross section). In future it might be possible to define each plate pair individually.

Figure 13. Support plates results tab, KC Runway

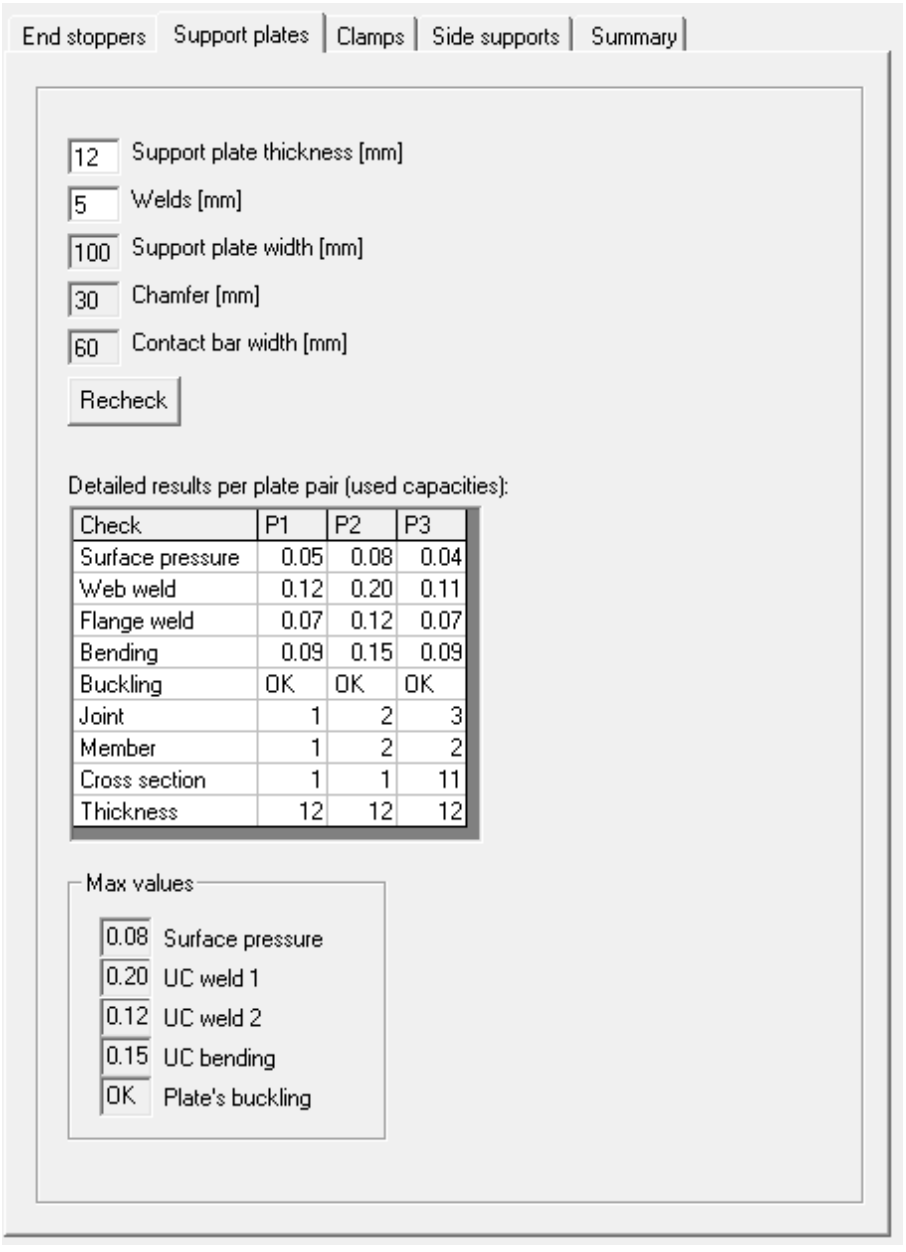

Check	P1	P2	P3
Surface pressure	0.05	0.08	0.04
Web weld	0.12	0.20	0.11
Flange weld	0.07	0.12	0.07
Bending	0.09	0.15	0.09
Buckling	OK	OK	OK
Joint	1	2	3
Member	1	2	2
Cross section	1	1	11
Thickness	12	12	12

4.2.6 Optimisation

When the plate fails the buckling check, but the compressive strength used capacity of the plate is relatively small, there are certain conditions in which lowering the assumed plate's yield strength might be beneficial for the buckling check. The following example calculation in Mathcad illustrates this situation:

$t_w := 16.5\ mm$	thickness of the web plate	$f_y := 355\ MPa$
$t_f := 31\ mm$	thickness of the flange	$\gamma_{M0} := 1.1$
$k := 30\ mm$	chamfer	$F_{EdvA} := 480\ kN$
$b_p := 130\ mm$	depth of the web plate	
$t_p := 10\ mm$	support plate thickness	
$b_{bar} := 50\ mm$	width of the support bar	

$$\varepsilon := \sqrt{\frac{235\ MPa}{f_y}} = 0.814 \qquad \frac{b_p}{t_p} = 13 \qquad 14 \cdot \varepsilon = 11.391$$

$$\text{Buckling} := \text{if}\left(\left(\frac{b_p}{t_p} \le 14 \cdot \varepsilon\right), \text{“OK”}, \text{“NOK”}\right) = \text{“NOK”}$$

Surface pressure:

$$\sigma_{Rd} := \frac{f_y}{\gamma_{M0}} = 322.727\ MPa$$

$$A_c := b_{bar} \cdot \left(t_w + 2 \cdot t_f\right) + \left(b_p - k\right) \cdot t_p \cdot 2 = \left(5.925 \cdot 10^3\right)\ mm^2$$

$$\sigma_{Ed} := \frac{F_{EdvA}}{A_c} = 81.013\ MPa$$

$$UC := \frac{\sigma_{Ed}}{\sigma_{Rd}} = 0.251$$

In this example, the used capacity for the surface pressure is low, but the plate has to be rejected due to the failed buckling check. However, if lower yield strength of the plate is assumed, with all the other inputs unchanged, the plate passes the buckling check and can be accepted, despite increased used capacity, as illustrated below:

$$f_y := 235\ \boldsymbol{MPa}$$

$$\varepsilon := \sqrt{\frac{235\ \boldsymbol{MPa}}{f_y}} = 1 \qquad 14 \cdot \varepsilon = 14$$

$$\mathbf{Buckling} := \mathbf{if}\left(\left(\frac{b_p}{t_p} \leq 14 \cdot \varepsilon\right), \text{“OK”}, \text{“NOK”}\right) = \text{“OK”}$$

Surface pressure:

$$\sigma_{Rd} := \frac{f_y}{\gamma_{M0}} = 213.636\ \boldsymbol{MPa}$$

$$UC := \frac{\sigma_{Ed}}{\sigma_{Rd}} = 0.379$$

As indicated, the used capacity increases, but it is still well within the limit, whereas the buckling check in this case is accepted.

It must be noted that the real savings from this approach in the case of support plates for a single runway beam are not very significant compared to the whole runway. However, in the scale of the whole European business, savings from this simple tweak could reach tens of tonnes of steel per year in optimal conditions.

4.3 Clamps

4.3.1 Description and purpose

Clamps are used to hold the runway in place on the supports and prevent tipping over the runway under the horizontal transverse load (Figure 14). In one of the basic forms, they are made from a simple steel plate cut into shape as in the Figure 15. The clamps are welded to a contact bar, which is located laterally under the runway and acts as a direct support and a pivot point for the runway. There are two types of clamps: locking clamps and non-locking clamps. The difference is that the former also prevents the runway from moving in the longitudinal direction (X axis) by being welded to the bottom flange of the runway as well as to the contact bar under the runway. Typically, there is one pair of locking clamps per runway and it is located in the middle of the runway's total length, unless expansion joints are used – in which case a pair of locking clamps is needed per each independent section of the runway.

Figure 14. Cross section of a runway beam with clamps and forces marked.

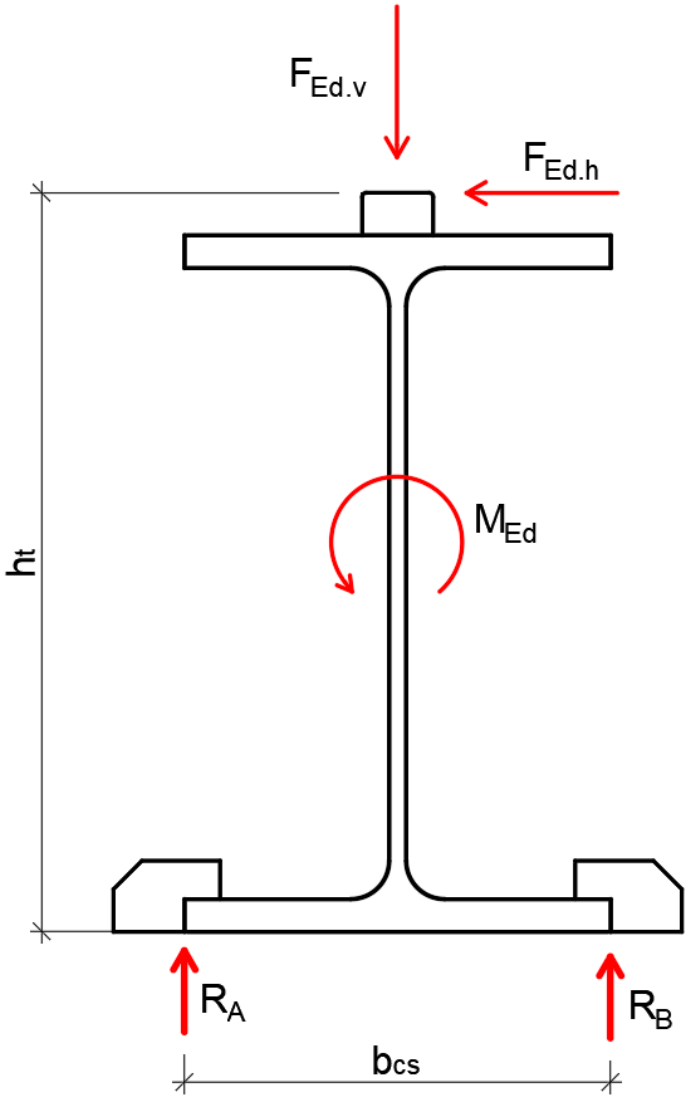

Figure 15. Runway clamp.

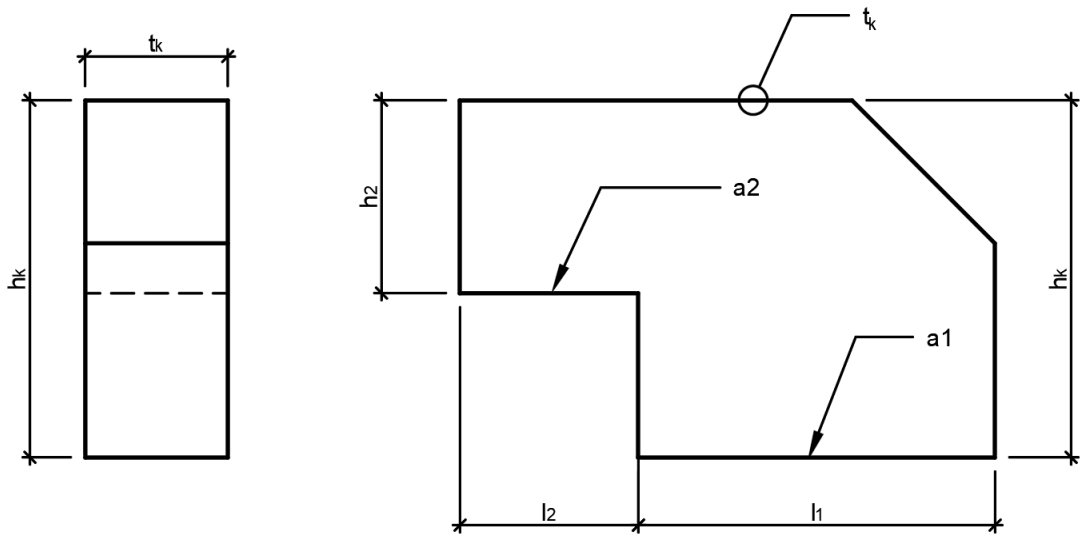

4.3.2 Analysis and loads acting

It is essential to consider different load scenarios when outlining the clamps securing the runway to the consoles. In this section, the load scenarios critical to the clamp design and the relevant forces for each scenario will be discussed.

There are three distinct load scenarios to be considered in the clamp design:

- Case 1 - The crane's trolley is parked in close proximity to the clamps, resulting in the maximal vertical force (F_v)

- Case 2 - The crane's trolley is parked the farthest away from the clamps, close to the other end of the crane bridge, causing F_v to be negligible and assumed as zero

- Case 3 - Applies to cranes in which the runway's terminal spans extend over their supports, effectively creating a cantilever, where F_v at a support located one span away may be negative (uplift).

It is important to note that a thorough examination of Case 1 and Case 2 is always required, whereas Case 3 is only necessary for cantilever designs.

In terms of clamp types, there are two primary classifications, as mentioned before: locking clamps (LC) and non-locking clamps (NLC). Typically, one set of locking clamps per runway is installed, unless expansion joints are used.

For each locking clamp, a total of three calculations are needed: top weld (Figure 15, weld a2), bottom weld (Figure 15, weld a1), and plate tearing. In contrast, non-locking clamps require only two calculations, as there is no top weld involved. The total number of calculations for both types of clamps in all three scenarios is 3 x 3 (LC) + 3 x 2 (NLC) = 15. To expedite the design process, it is beneficial to identify the critical calculations.

Since non-locking clamps do not have top welds, the top weld calculations will necessarily be derived from locking clamps. Regarding the plate tearing calculations, LCs will always be more critical or at least equal to NLCs due to the presence of both the same forces (horizontal and vertical) and an additional axial force. However, for the bottom weld calculations, both types of clamps need to be verified for the reason that while the LCs involve additional axial force which NLCs do not (alongside the horizontal and vertical forces present in non-locking clamps), the resultant force is divided between the two clamps. In contrast, for the non-locking clamp the horizontal force must be absorbed entirely by a single clamp, therefore it is possible that the resulting utilisation ratio is higher.

Furthermore, analysing the three load scenarios, it is evident that the maximum vertical force (F_v) will have a favourable impact on clamp design. This is because it acts as a stabilizing force against the uplift generated by the horizontal force (attributable to the created moment, see Figure 14). This implies that assuming F_v to be zero, as in Case 2, represents the worst-case scenario. For cantilever designs, if an uplift occurs, it becomes the most unfavourable case. If no uplift occurs, then $F_v = 0$ remains the worst case. Consequently, among the 15 potential calculations, only four are essential if F_v is either assumed to be zero at most, or negative in the case of a cantilever design.

It should be acknowledged that there exists an additional loading scenario, which, although theoretically possible, is not explicitly calculated due to its extremely low probability and brief acting time. This particular scenario involves an accidental situation where the full hoisting load is abruptly released from the hook, perhaps as a result of a malfunction. In such an event, the sudden release of the potential energy stored in the form of elastic tension, mainly within the rope and the crane's main girders, could cause girders to rapidly accelerate upwards and lift the end carriages. If the crane were to be equipped with an anti-jump (catch) system, this acceleration would be transferred to the runway, and subsequently to the clamps. However, in practical terms, this scenario is highly improbable, and it is generally presumed that the weight of both the main girders and the runway would serve to prevent any uplift from occurring.

4.3.3 Calculations

Support reactions

First, calculating the support reactions under the cross section of the runway beam, R_A and R_B:

$$R_A = \frac{M_{Ed} + F_{Ed.h} * h_t + \frac{F_{Ed.v}}{2} * b_{cs}}{b_{cs}} \quad (42)$$

$$R_B = F_{Ed.v} - R_A \quad (43)$$

Where M_{Ed} is the moment around the x axis (e.g. from the side platform), $F_{Ed.h}$ is the resulting horizontal force (skewing, lateral acceleration etc), h_t is the hight from the support bar to the top of the rail, b_{cs} is the width of the beam and $F_{Ed.V}$ is the vertical load.

Bottom weld a1 (the so-called foot weld) in a locking clamp

The contributing forces are the following:

- Vertical, in case there is any uplift, otherwise it's zero (worst case scenario)
- Horizontal (skewing, etc)
- Axial, including the buffer collision force

The same limitations about the minimum dimensions of the welds apply as in chapter 5.1.2, paragraph "Welds resistance". Likewise, the following equations allow to calculate the used capacity of the bottom weld a_1 of the locking clamp, this time in accordance with the simplified method given in the Eurocode 3 (EN 1993-1-8:2005, 2005, p. 44):

$$F_{Rd.a1} = \frac{2 * a_1 * l_{eff} * f_u}{\gamma_{M0} * \sqrt{3} * \gamma_{M2}} \quad (44)$$

$$F_{Ed.t} = \sqrt{\left(\frac{F_{Ed.h}}{2}\right)^2 + \left(\frac{F_{Ed.buff} + F_{Ed.x}}{2}\right)^2 + min(R_A, R_B, 0)^2} \quad (45)$$

$$UC = \frac{F_{Ed.t}}{F_{Rd.a1}} \quad (46)$$

Alternatively, the directional method discussed earlier can also be used:

$$\tau_{\parallel} = \frac{F_h}{2 * a_1 * l_{eff}} \quad (47)$$

$$\sigma_{\perp} = \frac{F_v + F_{ax}}{2 * a_1 * l_{eff} * \sqrt{2}} \quad (48)$$

$$\tau_{\perp} = \frac{F_{ax}}{2 * a_1 * l_{eff} * \sqrt{2}} \quad (49)$$

$$UC = \frac{\sqrt{{\sigma_{\perp}}^2 + 3 * \left({\tau_{\perp}}^2 + {\tau_{\parallel}}^2\right)}}{\frac{f_u}{\beta_w * \gamma_{M2}}} \quad (50)$$

Where F_h is the horizontal force, F_v is half of the vertical force in case of an uplift (because of two clamps per console) or 0 otherwise, and F_{ax} is the combination of the axial force and the buffer impact force.

The simplified method gives slightly more conservative results, as expected.

In addition, it is possible to calculate the minimum size of the welds from the capacity perspective for the same size clamp (keeping in mind the previously mentioned limitations of l_{eff}):

$$a_{min} = \sqrt{\left(\frac{F_v + F_{ax}}{2 * l_{eff} * \sqrt{2}}\right)^2 + 3 * \left(\left(\frac{F_{ax}}{2 * \sqrt{2} * l_{eff}}\right)^2 + \left(\frac{F_h}{2 * l_{eff}}\right)^2\right)} * \frac{\beta_w * \gamma_{M2}}{f_u} \quad (51)$$

Bottom weld a1 in a non-locking clamp

The bottom weld for the non-locking clamp is calculated analogously with the only difference that the horizontal force is distributed over a smaller weld area, corresponding to a single clamp, and axial force is not considered at all.

$$F_{Rd.a1} = \frac{2 * a_1 * l_{eff} * f_u}{\gamma_{M0} * \sqrt{3} * \gamma_{M2}} \quad (52)$$

$$F_{Ed.t} = \sqrt{(F_{Ed.h})^2 + \min(R_A, R_B, 0)^2} \quad (53)$$

$$UC = \frac{F_{Ed.t}}{F_{Rd.a1}} \quad (54)$$

Top weld a2 (the so-called hook weld)

For the top weld, the contributing forces are the following:

- Horizontal Fy (skewing, etc)
- Axial Fx, including the buffer collision force

The vertical force *Fz* is not considered because if it acts downward, it is transferred directly to the console (causing a support reaction) so it is irrelevant for the weld, and if it creates an uplift, it might interact with the clamp's top hook part from the bottom directly through surface contact. Subsequently, the following equations apply:

$$F_{Rd.a2} = \frac{2 * a_2 * l_{eff2} * f_u}{\gamma_{M0} * \sqrt{3} * \gamma_{M2}} \quad (55)$$

$$F_{Ed.t} = \sqrt{\left(\frac{F_{Ed.h}}{2}\right)^2 + \left(\frac{F_{Ed.buff} + F_{Ed.x}}{2}\right)^2} \quad (56)$$

$$UC = \frac{F_{Ed.t}}{F_{Rd.a2}} \quad (57)$$

Plate tearing – combined shear, bending and axial force

As discussed earlier, the most critical loading situation for clamp's shear resistance will happen for a locking clamp when all three force components are present. The forces are transferred to the clamp through its weld a_2 which causes eccentricities in relation to the centre of the top, hooking part of the clamp. Therefore, each force will also produce a bending moment, three in total, which need to be considered in the calculations in addition to the shear stress. This is shown in graphical form in Figure 16. Additionally, from the clamp's smallest cross-section perspective (marked in red dashed line in the figure), force $F_{Ed.h}$ acts like a tensile axial force. In summary, there are stresses present due to shear, bending and tension simultaneously that need to be combined and the critical point evaluated. The European standard allows using von Mises general plane stress yield criterion for that purpose (EN 1993-1-1:2022en, 2022, p. 57):

$$\frac{\sqrt{\sigma_{x,Ed}^2 + \sigma_{z,Ed}^2 - \sigma_{x,Ed}^2\sigma_{z,Ed}^2 + 3 * \tau_{Ed}^2}}{f_y/\gamma_{M0}} \leq 1 \quad (58)$$

where:

$\sigma_{x,Ed}$ is the design value of the longitudinal normal stress

$\sigma_{z,Ed}$ is the design value of the transverse normal stress

τ_{Ed} is the design value of the shear stress

Figure 16. Forces acting on the clamp, eccentricities and resulting bending moments.

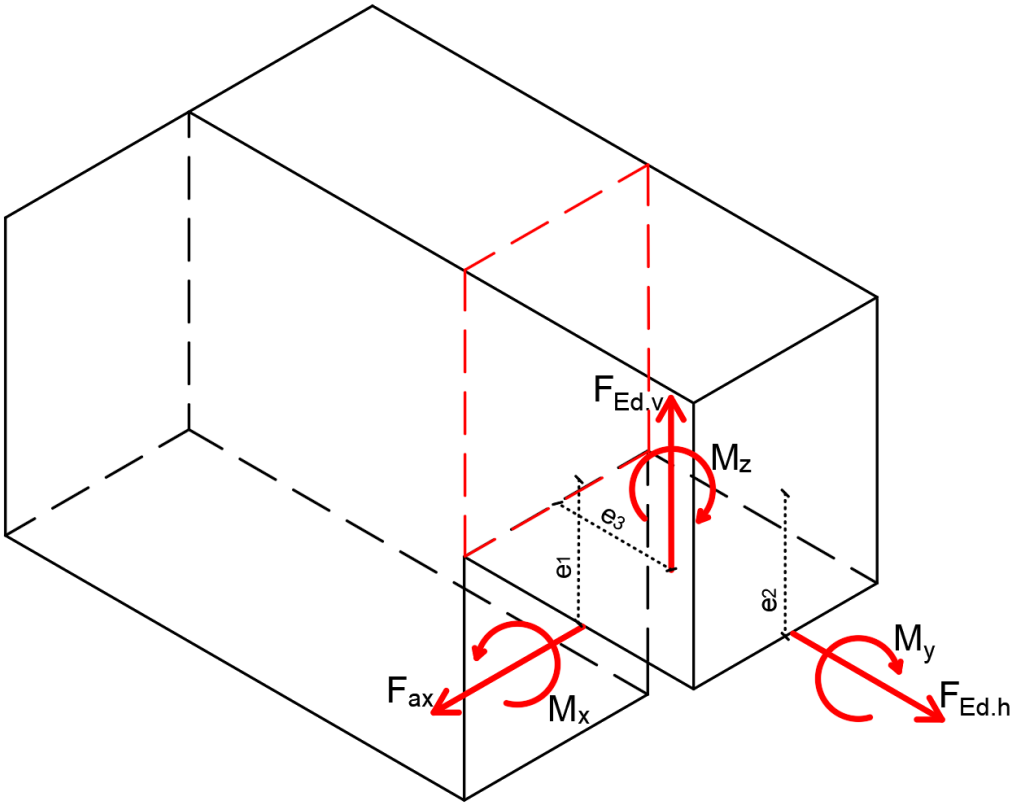

In case of the clamps there is no transverse normal stress. The point of consideration should be the most critical point where the stresses are the highest. It is assumed that the shear stress will be the highest in the centre of the cross section because there are two shear forces acting in one plane but at 90 degrees in relation to each other (Zhuravskii formula). It should be noted that in reality the shear distribution will probably be more complex, therefore some assumptions and simplifications are inevitable when using only analytical formulas.

The highest longitudinal normal stress due to biaxial bending can be assumed to be in one of the corners, whereas the normal stress due to the axial force is assumed to be evenly distributed over the whole surface. The two normal stresses (from bending and from axial force) can be added directly since they act in the same direction.

This results in the highest normal stress in one of the corners of the cross section, and highest shear stress in the middle (Figure 17). To locate the maximum resulting equivalent von Mises stress (under the assumptions mentioned earlier), the two functions must be combined and its maximum calculated. Alternatively, the maximum values of the normal stress and the shear stress can be used in the equation (58) which will result in a conservative design.

Figure 17. Distribution of stresses (z-axis) in 3D in the clamp cross section (x- and y-axis). Combined normal stress in black, shear stress in blue.

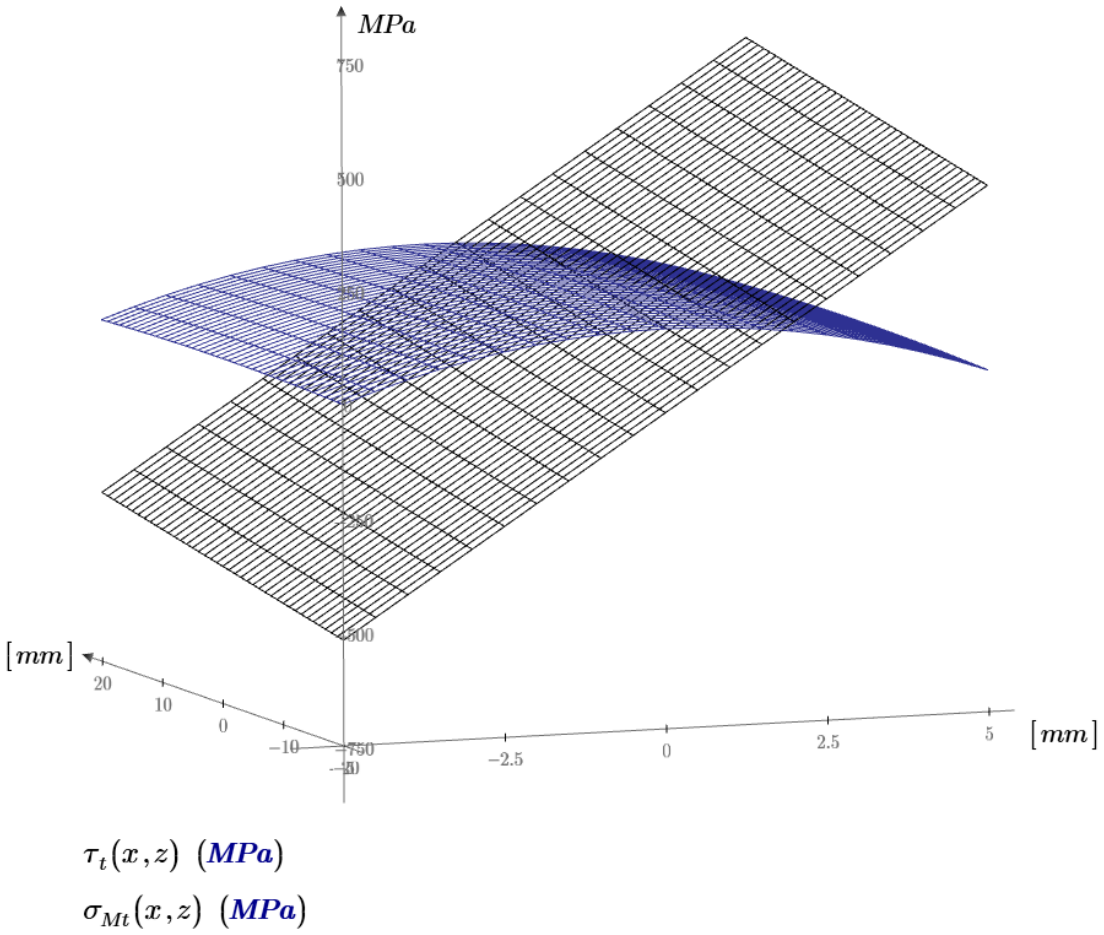

Shear stress

To calculate the shear stress, first moment of an area of the cross-section *Q* must be calculated in both directions *x* and *z* followed by the moment of inertia I. Then the shear stress at the neutral axis can be obtained using the general equation:

$$\tau = \frac{V * Q}{I * t} \tag{59}$$

where V is the shear force in each direction and t is the horizontal width of the cross section at the point of interest.

Bending moment

It is assumed that the forces are evenly distributed and transferred to the locking clamp through a pair of top welds and bending moments results from eccentricities of the loads applications. Specifically, $F_{Ed.V}$ and $F_{Ed.h}$ both cause bending around x-axis and $F_{Ed.x}$ causes bending around y-axis (Figure 16). The point of application is in the middle of the load distribution.

As an example, to calculate the normal stress due to bending moment caused by $F_{Ed.h}$ for a locking clamp:

$$M_h = \sqrt{\left(\frac{F_h}{2}\right)^2} * {}^{h}/_{2} \tag{60}$$

$$\sigma_{Mh} = \frac{M_h * z}{I} \tag{61}$$

Where I is the moment of inertia in appropriate direction and z is the distance to the farthest fibre from the neutral axis, in practice half of the width or the height of the “hook”. Other bending moments are calculated analogously. Full calculation example is shown in the Appendix 2.

It must be ensured that correct values of forces are used, noting that some forces are split between two clamps, like the longitudinal force $F_{Ed.x}$ in case of the locking clamps, whereas others are not, like the horizontal force $F_{Ed.h}$ in case of a non-locking clamp.

4.3.4 Optimisation

As was the case with the end stoppers, in the software it is possible to check a specific size of the clamps given by the user, or auto-select suitable size (including the welds).

The minimum dimensions according to the standard, as stated previously in chapter 4.1.2 Loadings involved, are:

- L_{eff} = 30mm
- Throat thickness a = 3mm

- Plate thickness t_k = 4mm

That means that the absolute minimum length of the clamp is 2x(30mm+2x3mm)=72mm.

Also, the minimum height of the clamp can be calculated from the plate shearing, provided that the plate thickness is known:

$$H_2 = \frac{\sqrt{\left(\frac{F_{Ed.h}}{2}\right)^2 + \left(\frac{F_{Ed.buff} + F_{Ed.x}}{2}\right)^2 + \min(R_A, R_B, 0)^2}}{\frac{t_k * f_y}{\sqrt{3} * \gamma_{M0}}} \quad (62)$$

The algorithm takes all those minimum values and checks the used capacities. If any check fails, the plate thickness, the weld size or the plate height is increased until a solution is found.

4.3.5 Implementation and results

The clamps calculations implemented into KC Runway are presented in Figure 18. All clamps are calculated at the same time using loads specific to each joint. In addition, the total height of the clamp is calculated automatically using the thickness of the lower flange of the runway profile calculated in an earlier step. It is also marked if a given clamp is locking or not.

Figure 18. Clamps results tab, KC Runway.

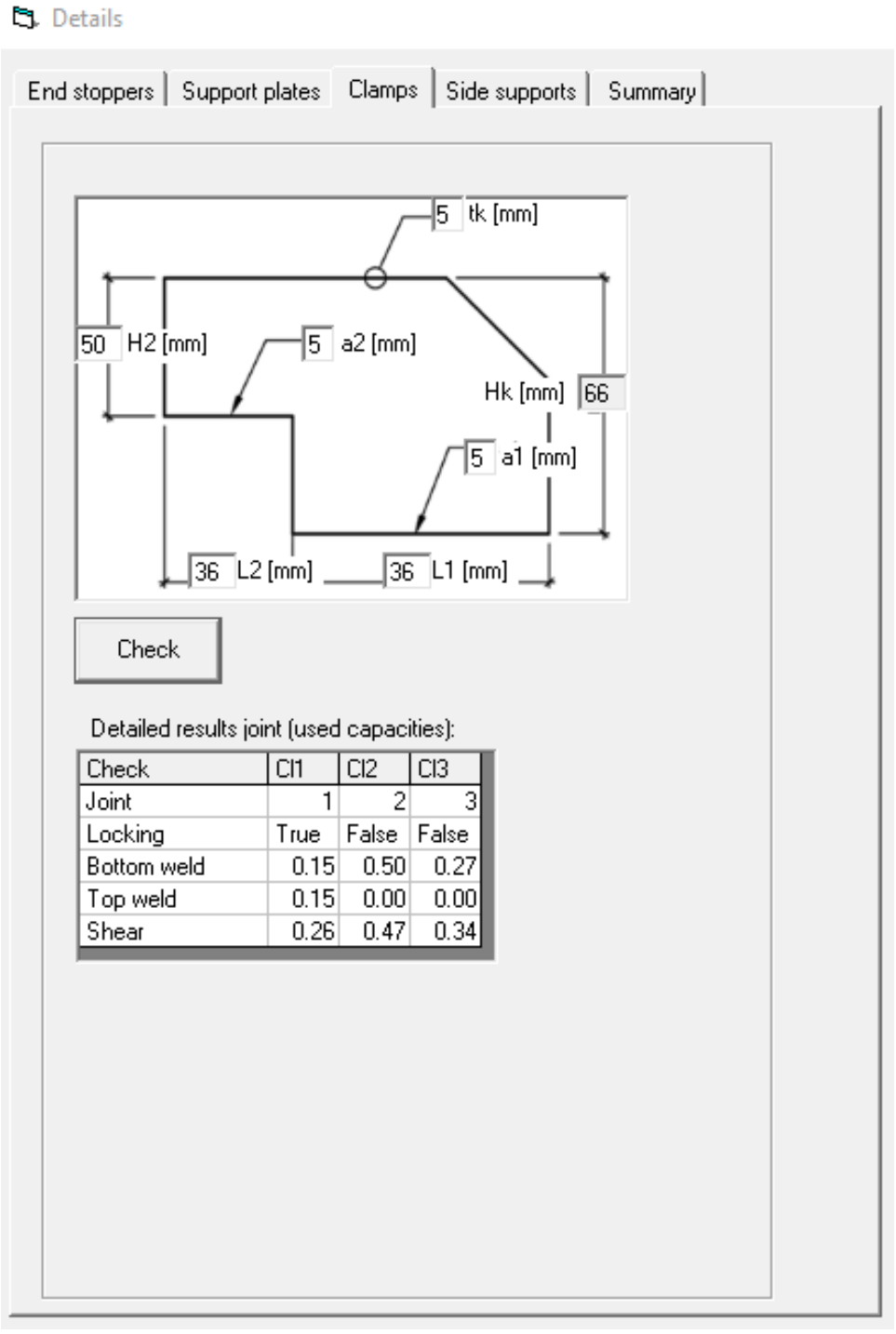

5 Further development

Following the successful completion of the thesis, the next phase of the development will involve addressing certain areas to further enhance the functionality and versatility of the runway design software. The identified areas for further analysis and development include:

- Adding support for other standards
  The expansion will allow broader applicability of the software thus allowing Konecranes to provide internally designed runways on other global markets.

- Adding bolted end stoppers and other profiles
  This enhancement will involve the development of bolted end stoppers as an alternative to welded ones, which will provide greater flexibility in the design and assembly of runway elements, facilitating ease of adjustment and modification during the lifetime of the structure. Moreover, additional profiles will increase the development flexibility.

- Adding side supports
  As an alternative to clamps, side supports are advantageous in certain situations.

- Adding underhung crane
  The software will be extended to include capabilities for designing runway elements that cater specifically to underhung crane configurations. This addition ensures comprehensive support for a wider range of crane types, accommodating more diverse needs of the customers.

- Adding column support
  The expansion will allow broader applicability of the software thus allowing Konecranes to provide internally designed runways on other global markets.

All these developments will greatly advance the capabilities of the software, making it a more robust and versatile tool for engineers involved in the design and calculation of crane runways. These improvements will cater to a broader spectrum of crane system configurations, thereby enhancing the software's utility in real-world engineering and offering applications.

6 Summary

This thesis is a part of a larger project aimed at updating the internal calculation software used within Konecranes with new functionality, namely calculating runway's structural details so that they can be easily and rapidly dimensioned, and thus quickly offered to the customers.

When analysing the existing calculation methods used in Konecranes and comparing to the standards and other sources, in two instances minor discrepancies were identified, having a marginal impact on the final outcomes. In one specific case, it was required to extend the calculations to incorporate additional checks, which allowed optimisation of the design.

The compiled knowledge consolidated in this thesis provides a solid and comprehensive theoretical foundation, on which the practical software development can now be continued. Furthermore, experience gained from partially implementing the calculations, optimisation algorithms and creating the user interface already at this stage will undoubtedly prove advantageous in the next stage of the project.

References

EN 1011-2. (2001). *European Standard: Welding - Recommendations for welding of metallic materials.* Helsinki: Finnish Standard Association SFS.

EN 13001-3-1:2012 + A2:2018. (2012). *Cranes. General Design. Part 3-1: Limit States and proof competence of steel structure.* Helsinki: Finnish Standard Association SFS.

EN 16851:2017 + A1:2020:en. (2020). *Light crane systems.* Helsinki: Finnish Standard Association SFS.

EN 1993-1-1:2022en. (2022). *Design of steel structures: General rules and rules for buildings.* Helsinki: Finnish Standard Association SFS.

EN 1993-1-5. (2006). *Plated structural elements.* Helsinki: Finnish Standard Association SFS.

EN 1993-1-8:2005. (2005). *Design of steel structures - Part 1-8: Design of joints.* Helsinki: Finnish Standard Association SFS.

Directive on machinery 42/EC/2006 http://data.europa.eu/eli/dir/2006/42/oj

Konecranes. (2016). *Single or double-girder crane? Konecranes experts help advise you on the right crane choice*. https://urly.fi/3wvU

Konecranes. (2024). *About Konecranes*. https://www.konecranes.com/about

Kubicki, K. (2021). The analysis of the resistance of tee joint fillet welds according to Eurocode 3. *Scientific Papers of the Częstochowa University of Technology*, 27 (177), 106-111. https://www.sbc.org.pl/dlibra/publication/edition/633157

Regulation on harmonised conditions for the marketing of construction products No 305/2011 http://data.europa.eu/eli/reg/2011/305/oj

SSAB. (2019). *Welding Handbook, ed.2.* SSAB.

Appendix 1. Example of an additional check for runway end stoppers

Additional check for runway end stoppers in cases of justified concerns about stiffness of the flanges. It is based on a simple check if the steel at the rail's weld location is sufficient to withstand the tension reaction due to the buffer collision forces.

Initial data

Buffer force	$F_b := 13\ kN$
Yield strength	$f_y := 355\ MPa$
Crane buffer height	$h_b := 100\ mm$
End stopper web height	$E_w := 120\ mm$
Partial safety factors	$\gamma_{Qsup} := 1.35$
	$\varphi_7 := 1.25$
Weld throat thickness	$a_1 := 5\ mm$
End stopper profile thickness	$t := 4\ mm$
Rail's width	$b_{rail} := 50\ mm$

Used capacity

Buffer design force	$F_{EdB} := F_b \cdot \varphi_7 \cdot \gamma_{Qsup} = 21.938\ kN$
Effective lenght of the weld	$l := b_{rail}$
	$l_{eff} := l - 2 \cdot a_1 = 40\ mm$
Design resistance of the steel at the weld location	$F_{Rd} := f_y \cdot l_{eff} \cdot t = 56.8\ kN$
Tension force at that location (one of the reactions, Fig. 4)	$F_{Ed.t} := \frac{F_{EdB} \cdot h_b}{E_w} = 18.281\ kN$
Used capacity	$UC := \frac{F_{Ed.t}}{F_{Rd}} = 0.322$

Appendix 2. Partial safety factors for γ_M

Resistance of members and cross-sections	γ_{M0} , γ_{M1} and γ_{M2} see EN 1993-1-1
Resistance of bolts	γ_{M2}
Resistance of rivets	
Resistance of pins	
Resistance of welds	
Resistance of plates in bearing	
Slip resistance - at ultimate limit state (Category C) - at serviceability limit state (Category B)	 γ_{M3} $\gamma_{M3,ser}$
Bearing resistance of an injection bolt	γ_{M4}
Resistance of joints in hollow section lattice girder	γ_{M5}
Resistance of pins at serviceability limit state	$\gamma_{M6,ser}$
Preload of high strength bolts	γ_{M7}
Resistance of concrete	γ_c see EN 1992

NOTE: Numerical values for γ_M may be defined in the National Annex. Recommended values are as follows: $\gamma_{M2} = 1{,}25$; $\gamma_{M3} = 1{,}25$ and $\gamma_{M3,ser} = 1{,}1$; $\gamma_{M4} = 1{,}0$; $\gamma_{M5} = 1{,}0$; $\gamma_{M6,ser} = 1{,}0$; $\gamma_{M7} = 1{,}1$.

Appendix 3. Mathcad calculation example for clamps

Full example of clamps calculations and comparison of previously used method (max allowable force and max allowable shear stress calculated separately vs stresses due to all components combined using von Mises criterion)

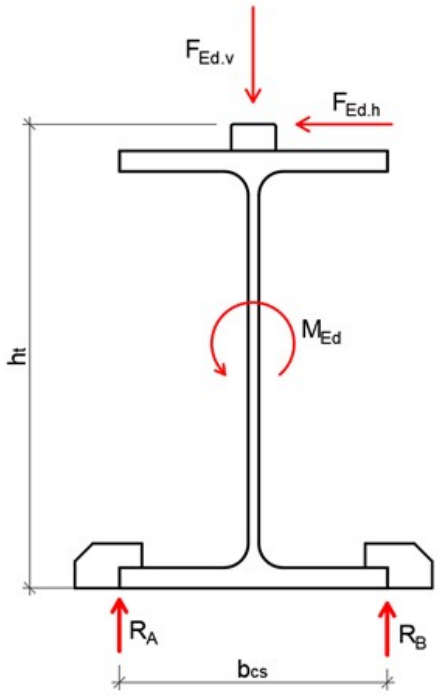

Initial data

Vertical design force (y)	$F_{Ed.V} := 61\ kN$
Horizontal (lateral) design force (z)	$F_{Ed.h} := 4.68\ kN$
Longitudinal design force (x)	$F_{Ed.x} := 0.95\ kN$
Additional moment around x	$M_{Ed} := 0\ kN \cdot m$
Buffer design force	$F_{Ed.buff} := 0\ kN$
Yield strength	$f_y := 355\ MPa$
Ultimate strength	$f_u := 520\ MPa$
Partial safety factors	$\gamma_{M0} := 1.1$
	$\gamma_{M2} := 1.25$

Dimensions

Distance from runway bottom to rail top	$h_t := 260\ mm$
Lower flange width	$b_{cs} := 220\ mm$
Clamp thickness	$tk := 10\ mm$
Total clamp height	$h_k := 71\ mm$
Clamp "hook" height	$h_2 := 50\ mm$
Clamp weld throat a1	$a_1 := 3\ mm$
Clamp weld throat a2	$a_2 := 3\ mm$
Clamp weld a1 length	$l_1 := 36\ mm$
Clamp weld a2 length	$l_2 := 36\ mm$

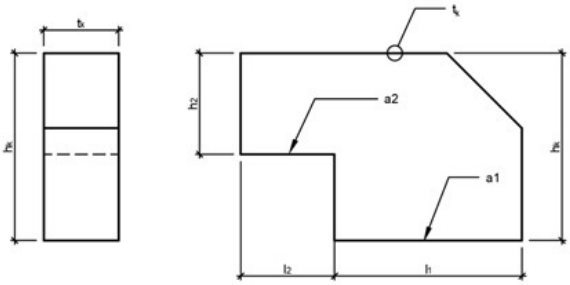

Reactions on the clamps*

$$R_A := \frac{\left(M_{Ed} + F_{Ed.h} \cdot h_t + \frac{F_{Ed.V}}{2} \cdot b_{cs}\right)}{b_{cs}} = 36.031\ kN$$

$$R_B := F_{Ed.V} - R_A = 24.969\ kN$$

*Directions: negative means uplift, i.e. tension in at least one clamp

Max force method

Quick and simplified method using force resultant, not recommended for this application

$$F_{Rd.H2} := \frac{h_2 \cdot tk \cdot f_y}{\sqrt{3} \cdot \gamma_{M0}} = 93.163\ kN$$

$$F_{Ed.tot} := \sqrt{\left(\left(\frac{F_{Ed.h}}{2}\right)^2 + \left(\frac{F_{Ed.buff} + F_{Ed.x}}{2}\right)^2 + min\left(R_A, R_B, 0\right)^2\right)} = 2.388\ kN$$

$$UC_{sh.HB} := \frac{F_{Ed.tot}}{F_{Rd.H2}} = 0.026$$

Max stress method

All stress components combined in Von Mises criterium and comparison to shear stress only.

$h := h_2 = 50\ mm$ $\quad b := tk = 10\ mm$

$F_v := min\left(\frac{F_{Ed.V}}{2}, 0\ kN, min\left(R_A, R_B\right)\right) = 0\ kN$ — *F vertical (i.e. transverse, neg = uplift)*

$F_h := F_{Ed.h}$ — *F horizontal (lateral)*

$F_{ax} := F_{Ed.buff} + F_{Ed.x}$ — *F axial (longitudinal), including buffer collision force*

Shear stress only

$$V := \sqrt{\left(\frac{F_{ax}}{2}\right)^2 + \left(\frac{F_v}{2}\right)^2} = 0.475\ kN$$

$Q(c) := \left(\frac{h}{2} - |c|\right) \cdot b \cdot \left(\frac{|c|}{2} + \frac{h}{4}\right)$ — *First moment of an area as distance c from N.A.*

$I := \frac{b \cdot h^3}{12} = \left(1.042 \cdot 10^5\right)\ mm^4$

-h/2 < c < h/2 $\quad t := tk$

$\tau(c) := \frac{V \cdot Q(c)}{I \cdot t}$ $\quad c := \left(-\frac{h}{2}\right), \left(-\frac{h}{2} + 0.05\ mm\right) .. \left(\frac{h}{2}\right)$

$\tau_{max} := \tau(0) = 1.425\ MPa$

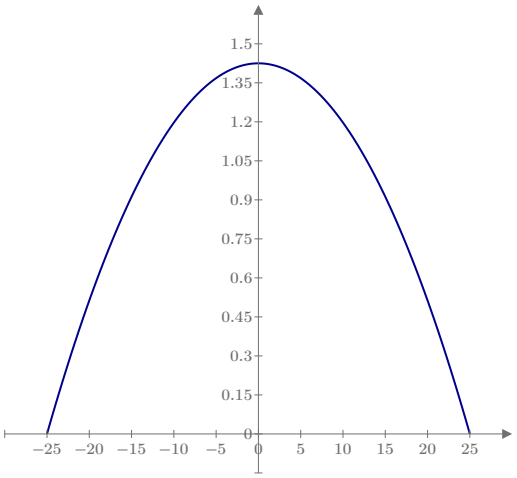

$\tau(c)\ \ (MPa)$

$c\ \ (mm)$

$$\tau_{avg} := \frac{\int_{-\frac{h}{2}}^{\frac{h}{2}} \tau(c)\,dc}{h} = 0.95\ MPa$$

$$UR := \frac{\tau_{max}}{\frac{f_y}{\sqrt{3}} \cdot \gamma_{M0}} = 0.006$$

Von Mises criterium - all stresses combined

von Mises equations
$\sigma_v = \sqrt{\frac{1}{2}\left[(\sigma_{11}-\sigma_{22})^2 + (\sigma_{22}-\sigma_{33})^2 + (\sigma_{33}-\sigma_{11})^2\right] + 3\left(\sigma_{12}^2 + \sigma_{23}^2 + \sigma_{31}^2\right)}$

Assumed directions:

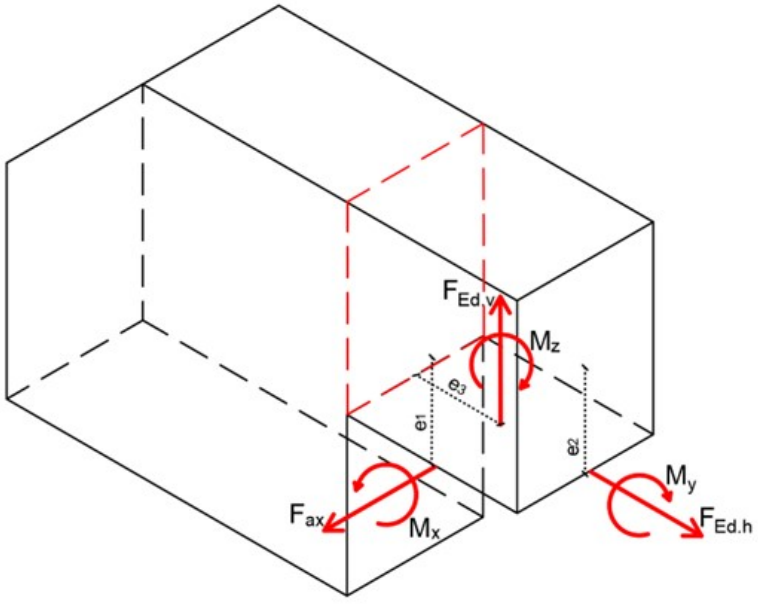

Normal stresses due to moments

Max stress due to moment caused by uplift (F_v)

$$M_x := |F_v| \cdot \frac{l_2}{2} = 0\ \boldsymbol{N \cdot m}$$

$$z := \frac{h}{2 \cdot \boldsymbol{mm}} = 25$$

$$\sigma_{Mx} := \frac{M_x \cdot z \cdot \boldsymbol{mm}}{I} = 0\ \boldsymbol{MPa}$$

Max stress due to moment caused by F_ax

$$M_z := \frac{\sqrt{F_{ax}{}^2}}{2} \cdot \frac{l_2}{2} = 8.55\ \boldsymbol{N \cdot m}$$

$$x := \frac{b}{2 \cdot \boldsymbol{mm}} = 5$$

$$I_x := \frac{h \cdot b^3}{12} = \left(4.167 \cdot 10^3\right)\ \boldsymbol{mm}^4$$

$$\sigma_{Mz} := \frac{M_z \cdot x \cdot \boldsymbol{mm}}{I_x} = 10.26\ \boldsymbol{MPa}$$

Normal stress due lateral force (F_h)

$$\sigma_{Ny} := \frac{|F_h|}{2 \cdot h \cdot b} = 4.68\ \boldsymbol{MPa}$$

Max stress due to moment due to F_h

$$M_h := \sqrt{\left(\frac{F_h}{2}\right)^2} \cdot \frac{h}{2} = 58.5\ \boldsymbol{m \cdot N}$$

$$\sigma_{Mh} := \frac{M_h \cdot z \cdot \boldsymbol{mm}}{I} = 14.04\ \boldsymbol{MPa}$$

Normal stresses combined, total:

$$\sigma_t := \sigma_{Mz} + \sigma_{Mx} + \sigma_{Ny} + \sigma_{Mh} = 28.98\ \boldsymbol{MPa}$$

Functions used to plot the graphs below

$$\sigma_{Mx}(z) := \frac{M_x \cdot z}{I} \cdot \boldsymbol{mm}$$

$$\sigma_{Mz}(x) := \frac{M_z \cdot x}{I_x} \cdot \boldsymbol{mm}$$

$$\sigma_{Mh}(z) := \frac{M_h \cdot z}{I} \cdot \boldsymbol{mm}$$

$$\sigma_{Mt}(x, z) := \sigma_{Mx}(z) + \sigma_{Mz}(x) + \sigma_{Mh}(z) + \sigma_{Ny}$$

Total stress due to bending moments in relation to position

Shear stresses in both directions and combining them

$h := \frac{h_2}{mm} = 50$ $\quad b := \frac{tk}{mm} = 10$ *this is just MathCad trick needed for the 3D graphs*

$V_x := \sqrt{\left(\frac{F_{ax}}{2}\right)^2} = 0.475\ kN$ $\quad Q_x(x') := \left(\frac{b}{2} - |x'|\right) \cdot h \cdot \left(\frac{|x'|}{2} + \frac{b}{4}\right)$ $\quad I_x := \frac{h \cdot b^3}{12} = 4.167 \cdot 10^3$

$V_z := \sqrt{(F_v)^2} = 0\ kN$ $\quad Q_z(z') := \left(\frac{h}{2} - |z'|\right) \cdot b \cdot \left(\frac{|z'|}{2} + \frac{h}{4}\right)$ $\quad I_z := \frac{b \cdot h^3}{12} = 1.042 \cdot 10^5$

$\tau_x(x') := \frac{V_x \cdot Q_x(x') \cdot mm^3}{I_x \cdot t \cdot mm^4}$ $\quad \tau_x(0) = 7.125\ MPa$

$\tau_z(z') := \frac{V_z \cdot Q_z(z') \cdot mm^3}{I_z \cdot t \cdot mm^4}$ $\quad \tau_z(0) = 0\ MPa$

Note: here Fv isn't divided by 2 clamps because it has been accounted for when calculating Fv above

$x := \frac{-b}{2}, \frac{-b}{2} + 0.5 .. \frac{b}{2}$ $\quad y := \frac{-b}{2}, \frac{-b}{2} + 1 .. \frac{b}{2}$ $\quad z := \frac{-h}{2}, \frac{-h}{2} + 1 .. \frac{h}{2}$

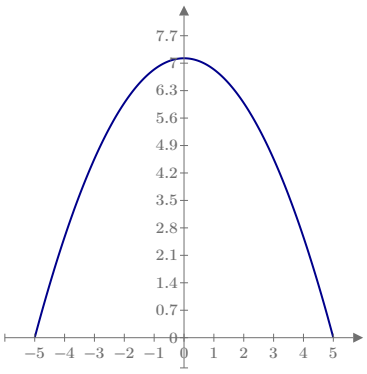

$\tau_x(x')$ (MPa)

x'

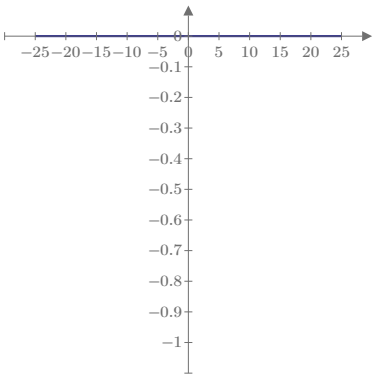

$\tau_z(z')$ (MPa)

z'

Combining both functions: $\tau_t(x, y) := \tau_x(x) + \tau_z(y)$

Shear stress and normal stress distributions in 3D

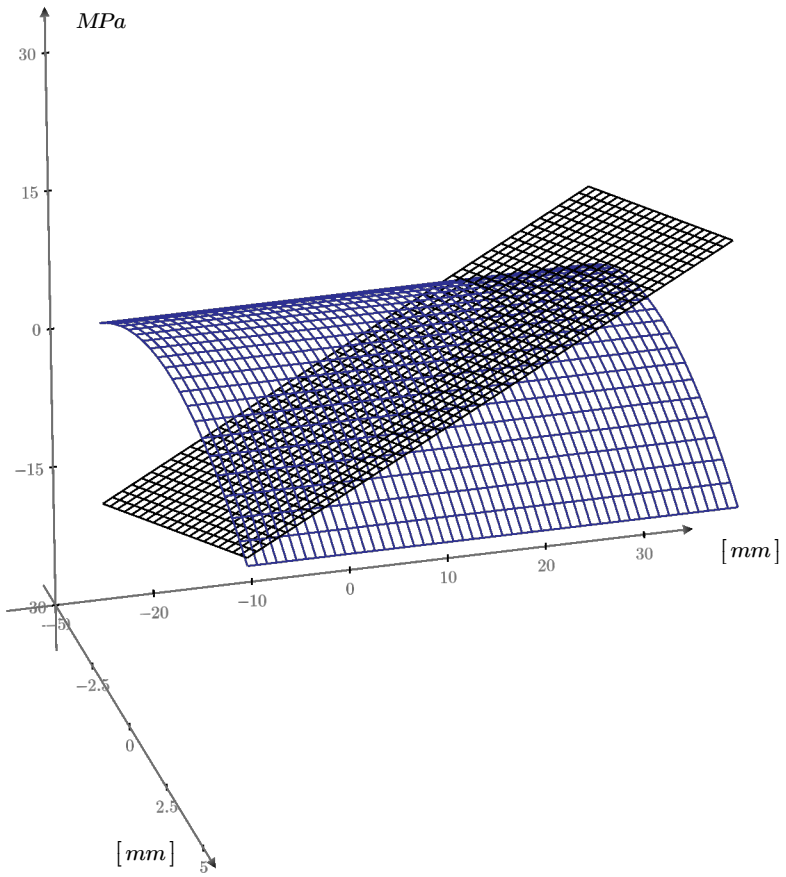

$\tau_t(x,z)$ **(MPa)**

$\sigma_{Mt}(x,z)$ **(MPa)**

Von Mises max shear + max normal: $\sigma_{vM} := \sqrt{\sigma_t{}^2 + 3 \cdot \left(\tau_t(0,0)^2\right)} = 31.498$ **MPa**

Von Mises function: $ft(x,y) := \sqrt{3 \cdot \left(\tau_t(x,y)^2\right) + \sigma_{Mt}(x,y)^2}$

All stresses combined shown in 3D

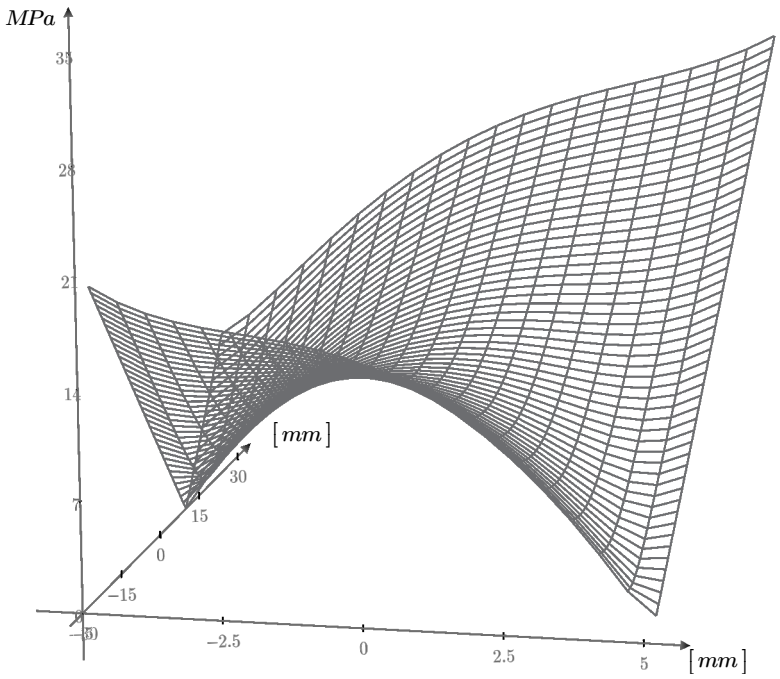

$ft(x,z)$ (MPa)

Testing points most likely to have biggest stress concentrations:

$$\sigma_{Eq} := \max\left(ft(0,0), ft\left(\frac{b}{2},\frac{h}{2}\right), ft\left(\frac{-b}{2},\frac{h}{2}\right), ft\left(\frac{b}{2},\frac{-h}{2}\right), ft\left(\frac{-b}{2},\frac{-h}{2}\right)\right) = 28.98\ MPa$$

Utilisation ratio when using the function:

$$UR := \frac{\sigma_{Eq}}{\frac{f_y}{\gamma_{M0}}} = 0.0898$$

Utilisation ratio when max values of stresses are used (conservative):

$$UR := \frac{\sigma_{vM}}{\frac{f_y}{\gamma_{M0}}} = 0.098$$